Cell Calcium xxx (2015) xxx–xxx

Contents lists available at ScienceDirect

Cell Calcium

journal homepage: www.elsevier.com/locate/ceca

Regionally diverse mitochondrial calcium signaling regulates spontaneous pacing in developing cardiomyocytes

Xiao-Hua Zhang[a], Hua Wei[a], Tomo Šarić[b], Jürgen Hescheler[b], Lars Cleemann[a], Martin Morad[a,*]

[a] Cardiac Signaling Center of USC, MUSC, & Clemson University, Charleston, SC, USA
[b] Institute for Neurophysiology, Medical Faculty, University of Cologne, Cologne, Germany

ARTICLE INFO

Article history:
Received 23 December 2014
Received in revised form 28 January 2015
Accepted 10 February 2015
Available online xxx

Keywords:
Pacing
Electrophysiology
Calcium
Ion channels
Mitochondria
Sarcoplasmic reticulum
Rat neonatal cardiomyocytes
Cardiomyocytes derived from human induced pluripotent stem cells
Genetically engineered fluorescent probes

ABSTRACT

The quintessential property of developing cardiomyocytes is their ability to beat spontaneously. The mechanisms underlying spontaneous beating in developing **c**ardio**m**yocytes are thought to resemble those of adult heart, but have not been directly tested. Contributions of sarcoplasmic and mitochondrial Ca^{2+}-signaling *vs.* I_f-channel in initiating spontaneous beating were tested in **h**uman **i**nduced **P**luripotent **S**tem cell-derived cardiomyocytes (**hiPS-CM**) and **r**at **N**eonatal cardiomyocytes (**rN-CM**). Whole-cell and perforated-patch voltage-clamping and 2-D confocal imaging showed: (1) both cell types beat spontaneously (60–140/min, at 24 °C); (2) holding potentials between −70 and 0 mV had no significant effects on spontaneous pacing, but suppressed action potential formation; (3) spontaneous pacing at −50 mV activated cytosolic Ca^{2+}-transients, accompanied by in-phase inward current oscillations that were suppressed by Na^+-Ca^{2+}-exchanger (NCX)- and ryanodine receptor (RyR2)-blockers, but not by Ca^{2+}- and I_f-channels blockers; (4) spreading fluorescence images of cytosolic Ca^{2+}-transients emanated repeatedly from preferred central cellular locations during spontaneous beating; (5) mitochondrial un-coupler, FCCP at non-depolarizing concentrations (~50 nM), reversibly suppressed spontaneous pacing; (6) genetically encoded mitochondrial Ca^{2+}-biosensor (mitycam-E31Q) detected regionally diverse, and FCCP-sensitive mitochondrial Ca^{2+}-uptake and release signals activating during I_{NCX} oscillations; (7) I_f-channel was absent in rN-CM, but activated only negative to −80 mV in hiPS-CM; nevertheless blockers of I_f-channel failed to alter spontaneous pacing.

1. Introduction

In studies exploring the mechanisms of cardiac pacemaking much attention has been focused on processes that underlie the slow diastolic depolarization, that in SA-nodal cells start at −60 mV and terminates with upstroke of the action potential mediated by Ca^{2+} current. The primary candidates for slow diastolic depolarization have been the activation of: (1) inward I_f current (HCN2 and HCN4 genes [1–5]); (2) inward Na^+-Ca^{2+} exchanger current (I_{NCX}) activated by release of Ca^{2+} from ryanodine receptor (RyR2) [6–8]; (3) turnoff of K^+ current in Purkinje fibers [9–11] and activation of Na^+-K^+ ATPase or leak-type inward current [12,13].

In considering the mechanisms of pacing, it is possible that one process may dominate in sino-atrial pacing while other mechanisms become critical in Purkinje fibers [9–11], or in developing myocytes and pathological conditions. But, it is also plausible that the robust, persistent heartbeat requires interactions of number of entrained Ca^{2+}- and membrane potential-dependent oscillators [14], which may be modulated by mechanical stimuli [15,16], mitochondrial Ca^{2+} fluxes [17,18], and oxidative stress [19].

We chose to examine spontaneous pacing in developing myocytes by quantifying their pacing frequency under control conditions and when action potential generation were prevented by voltage-clamping the cells at fixed holding potential of −50 mV, allowing pacing to be monitored through cell shortening, I_{NCX} oscillations, and cytosolic and mitochondrial Ca^{2+}-transients. After finding that generation of action potentials had little effect on pacing frequency, we proceeded to probe the role in Ca^{2+} signaling at

Abbreviations: HCN channel, hyperpolarization-activated cyclic nucleotide-gated channel; hiPS-CM, cardiomyocytes derived from human induced pluripotent stem cells; I_f, "funny" current through HCN channel; I_{NCX}, Na^+-Ca^{2+} exchanger current; miPS-CM, cardiomyocytes derived from mouse induced pluripotent stem cells; NCX, Na^+-Ca^{2+} exchanger; rN-CM, rat neonatal cardiomyocytes; RyR, ryanodine receptor; SR, sarcoplasmic reticulum.

* Corresponding author at: Cardiac Signaling Center of University of South Carolina, Medical University of South Carolina and Clemson University, MUSC, 68 President St, BEB 306, Charleston, SC 29425, USA. Tel.: +1 +843 876 2400; fax: +1 +843 792 4606; mobile: 1 +803 873 7113.
E-mail address: moradm@musc.edu (M. Morad).

http://dx.doi.org/10.1016/j.ceca.2015.02.003
0143-4160/

−50 mV to determine: (1) How robust were the Ca^{2+} oscillations in rN-CM and hiPS-CM; (2) How did they compare with SA-nodal Ca^{2+} oscillations, reported to rise at random sub-sarcolemmal locations and be suppressed by clamping the membrane potential [14,20], and (3) What were the contributions of mitochondria, where Ca^{2+} fluxes through mitochondrial Ca^{2+}-uniporter and the Na^{+}-Ca^{2+}-exchanger are suggested to buffer cytosolic Ca^{2+}, thereby modulating pacing frequency [17,18]. Others have suggested, however, that mitochondrial Ca^{2+} fluxes are too small to have significant effects on cellular Ca^{2+} signaling physiologically [21].

To address these issues we used two models of developing myocytes, rN-CM and hiPS-CM. Compared to adult rodent cardiomyocytes, neonatal myocytes are reported to have altered functional protein expression (increased I_{NCX} and T-type Ca^{2+} current and decreased I_{K1}, I_{Ks}, and I_{Kr} *etc.* [22]), which might predispose them to spontaneous pacing. In general, hiPS-CMs have an immature structure (rounded or polygonal shape, few myofibrils and z-lines) and electrophysiologically express lower levels of I_{K1} and I_{to}. Most cell-line colonies appear to contain myocytes with ventricular, atrial and nodal action potential phenotypes. In addition, variability between different hiPS-CM cell-lines is even larger driving the ongoing effort to guide cellular differentiation [23]. We have previously reported on the hiPS-CMs used in the present study and found their Ca^{2+}-signaling properties to be stable and dominated by I_{Ca}-triggered release of Ca^{2+} from the SR [24–26]. While both cell types continued to beat spontaneously under a broad range of experimental conditions, the critical role of subcellular Ca^{2+} signals was seen most clearly when they were dialyzed with Fluo-4, or infected with genetic probes targeted to RyR2 (GCamP6-FKBP [27]) or cytochrome-C (mitycam-E31Q [28]), and were voltage-clamped at −50 mV to prevent the activation of any voltage-gated ion channels, but allow activation of currents (I_{NCX}) generated by release of Ca^{2+}.

To suppress motion-induced imaging artifacts or possible mechanical feedback mechanisms, we used firmly attached cultured myocytes and, in addition, incubated the cells with blebbistatin to desensitize the myofilaments to Ca^{2+} [29]. The voltage-clamped myocytes were also dialyzed with 5 mM ATP to prevent exhausting them metabolically or when the mitochondrial un-coupler FCCP was used at concentrations (~50 nM) that only stimulates mitochondrial oxidative metabolism, without depolarizing the mitochondria [30].

This is the first study to compare the details of Ca^{2+} signaling in two different spontaneously beating developing cell-types. The data suggests that spontaneous beating in hiPS-CM or rN-CM is triggered by rhythmic Ca^{2+} oscillations that activate in-phase NCX-currents, are independent of I_f expression, brief (~1 min) suppression of I_{Ca}, or changes (~20 s) in holding potential, and point to cross-talk between SR and mitochondria as a critical pacing mechanism. Imaging showed no indication that cellular Ca^{2+} transients start as random mutually reinforcing local sub-sarcolemmal Ca^{2+} releases. Rather, they rose from preferred central location and spread throughout the cell in a repeatable pattern. Mitycam-E31Q signals confirmed the presence of substantial mitochondrial Ca^{2+} transients, but also showed unexpected regional diversity between peripheral mitochondria that sequestered Ca^{2+} (*Cf.* [18,30]), and peri-nuclear mitochondria that released Ca^{2+} accompanying the cytosolic Ca^{2+} transients.

2. Methods

2.1. General experimental approach

Experiments with spontaneously beating hiPS-CM [25,26] and rN-CM [26,31] cultures were carried out in accordance with national and institutional guidelines. The beating was examined at 24 and 35 °C in intact cells and in single cells that were voltage- or current-clamped in configurations where the membrane under the patch pipette was either subjected to amphotericin B perforation or ruptured to allow cell dialysis. Holding potentials of −50 or −60 mV were used to measure spontaneous oscillations in membrane current I_{NCX}, without activating other voltage-dependent channels, I_f and I_{Ca}. Ca^{2+} oscillations were recorded fluorometrically using dialyzing solutions with 0.1 mM Fluo-4 or transient expression of either FKBP-linked GCamP6 [27] or a novel mitochondrially targeted probe (mitycam-E31Q [28]).

2.2. Neonatal cardiomyocyte (rN-CM) isolation

Rat neonatal CMs (rN-CM) were isolated using an isolation kit from Worthington Biochemical Corporation (Lakewood, NJ). One to six day-old neonatal rats were decapitated and the beating hearts were surgically removed and placed in chilled Hank's Balanced Salt Solution (HBSS). The main vessels and atria were removed and the ventricles were minced with a razor blade to pieces <1 mm^3 that were incubated in HBSS with trypsin (50 μg/ml) for 14–16 h at 4 °C. The digestion was then arrested by exposure to trypsin inhibitor (200 μg/ml) for 20 min in 37 °C. Thereafter collagenase (100 U/ml) was used for 30 min to isolate single rN-CM, which were filtered through a cell strainer and centrifuged at 1000 rpm for 3 min. Cells were re-suspended in Dulbecco's Modified Eagle's Medium (DMEM) containing 10% fetal bovine serum (FBS) with 1% penicillin/streptomycin and 1% non-essential amino acids, plated on 100 mm dishes and placed in the incubator for 1–1.5 h to eliminate fibroblasts. rN-CM overall viability was ~80%. Isolated single rN-CM were plated onto non-treated glass cover slips and used for electrophysiological experiments.

2.3. Cultivation of hiPS cells and preparation of hiPS-CM

Human iPS-CMs were produced by transfecting somatic cells from a healthy control individual with a set of pluripotency genes (*OCT4*, *SOX2*, *cMYC*, and *KLF4*) [32]. The generation, cardiac differentiation and characterization of these cells have been reported [24–26].

2.3.1. Culture of undifferentiated human induced pluripotent stem (hiPS) cells

The hiPS cells were maintained on mitomycin C-treated murine embryonic fibroblasts (MEF) prepared in our laboratory in DMEM/F12 medium supplemented with Glutamax, 20% knockout serum replacer, 1% nonessential amino acids (NAA), 0.1 mM β-mercaptoethanol (βME, Invitrogen, Darmstadt, Germany), 50 ng/ml FGF-2 (PeproTech, Hamburg, Germany). Cells were passaged by manual dissection of hiPS cell colonies every 5–6 days.

2.3.2. Cardiac differentiation

Cardiac differentiation of hiPS cells was carried out on the murine visceral endoderm-like cell line END2, which was provided by C. Mummery (Leiden University Medical Center, The Netherlands) [33]. END2 cells were mitotically inactivated for 3 h with 10 μg/ml mitomycin C (Sigma–Aldrich Chemie GmbH, Munich, Germany) and 1.2×10^6 cells were plated on 6 cm dishes coated with 0.1% gelatin one day before initiation of hiPS cell differentiation. To initiate co-cultures, hiPS cell colonies were dissociated into clumps by using collagenase IV (Invitrogen, 1 mg/ml in DMEM/F-12 at 37 °C for 5–10 min). The differentiation was carried out in knockout-DMEM containing 1 mM L-glutamine, 1% NAA, 0.1 mM βME and 1% penicillin/streptomycin (100 U/ml and 100 μg/ml, respectively). The co-culture was left undisturbed at

Please cite this article in press as: X.-H. Zhang, et al., Regionally diverse mitochondrial calcium signaling regulates spontaneous pacing in developing cardiomyocytes, Cell Calcium (2015), http://dx.doi.org/10.1016/j.ceca.2015.02.003

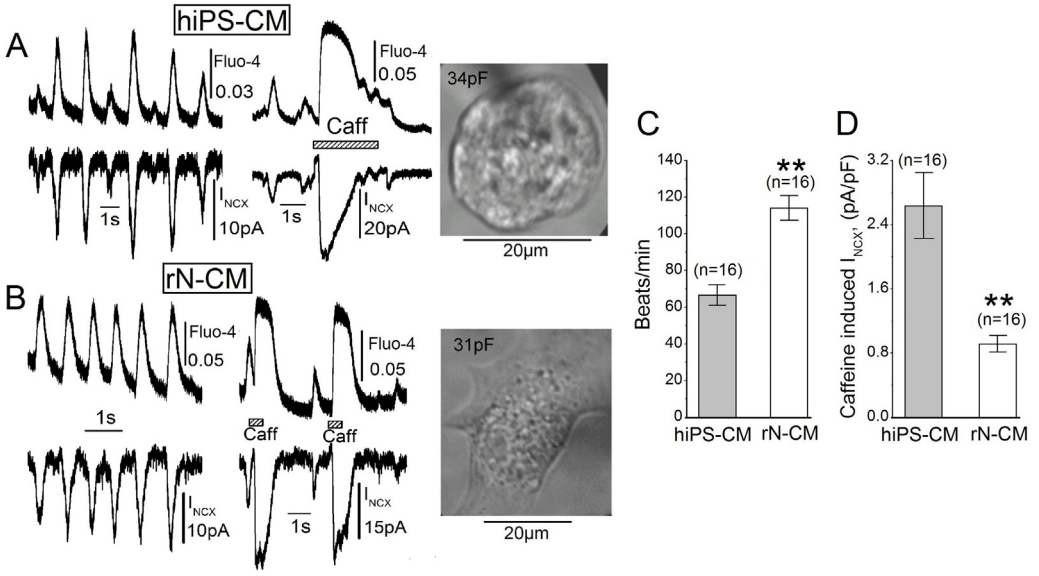

Fig. 1. Simultaneous measurements of I_{NCX} current and Ca^{2+}-signals in hiPS-CM (A) and rN-CM (B) voltage-clamped at −50 mV. (A) and (B) Signals during spontaneous beating (left) and exposure to 3 mM caffeine (middle) followed by microscopic bright field images of the voltage-clamped cell with labels indicating membrane capacitance (right). The bar graphs show differences in beating rate (C) and caffeine-induced I_{NCX} (D). Cells were voltage-clamped at 24 °C, and dialyzed with a solution containing 100 μM Fluo-4 to obtain whole-cell measurements of cytosolic Ca^{2+}.

37 °C/5% CO_2 for 5 days. Medium change was performed first on day 5 and later on days 9, 12 and 15 of differentiation.

2.3.3. Preparation of hiPS-CM for patch-clamp experiments

Beating areas were micro-dissected mechanically at day 40–45 of differentiation and dissociated with collagenase B. Single cardiomyocytes derived from hiPS cells (hiPS-CM) were then plated on fibronectin (2.5 μg/ml) -coated 12 or 25 mm glass cover slips and incubated for 36–72 h before their use in electrophysiological experiments.

2.3.4. Cardiomyocytes derived from mouse iPS cells

(miPSC-CM) were prepared by methods described previously [34,35] and were used in experiments probing the pacemaker current, I_f (Fig. 7). This iPS cell line (clone AT25) was genetically modified to express EGFP and puromycin resistance genes under the control of α-myosin heavy chain (α-MHC) promoter to enable visualization and generation of pure CM. For the purpose of this study, murine iPS-CMs were not subjected to antibiotic selection and were analyzed between days 35 and 40 of differentiation.

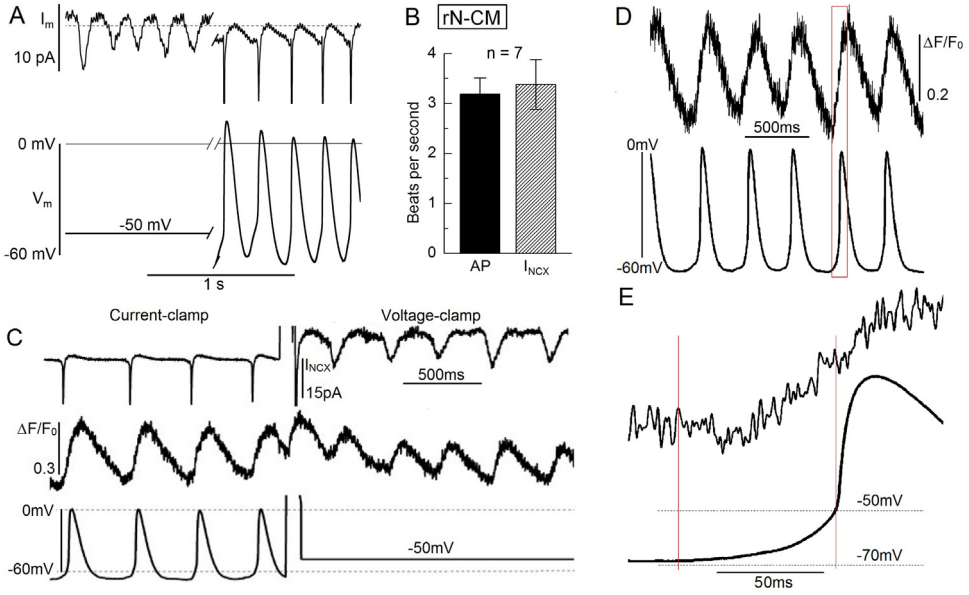

Fig. 2. Spontaneous beating in rN-CM measured at 35 °C in the perforated patch configuration. (A) and (C) Tracings of membrane current (I_m) and membrane potential (V_m) measured while rapidly switching back and forth between current- and voltage-clamp modes in cells without (A) or with Ca^{2+} measurements (C-E, $\Delta F/F_0$) using the biologically engineered Ca^{2+} probe GCamP6-FKBP. (B) Comparison of average beating frequency of action potentials (AP) and I_{NCX} transients in 7 cells without expression of GCamP6-FKBP. Panel E shows a single beat from panel D on an expanded time scale illustrating that the onset of the Ca^{2+} signal coincides with the diastolic depolarization that precedes the upstroke of the action potential.

Please cite this article in press as: X.-H. Zhang, et al., Regionally diverse mitochondrial calcium signaling regulates spontaneous pacing in developing cardiomyocytes, Cell Calcium (2015), http://dx.doi.org/10.1016/j.ceca.2015.02.003

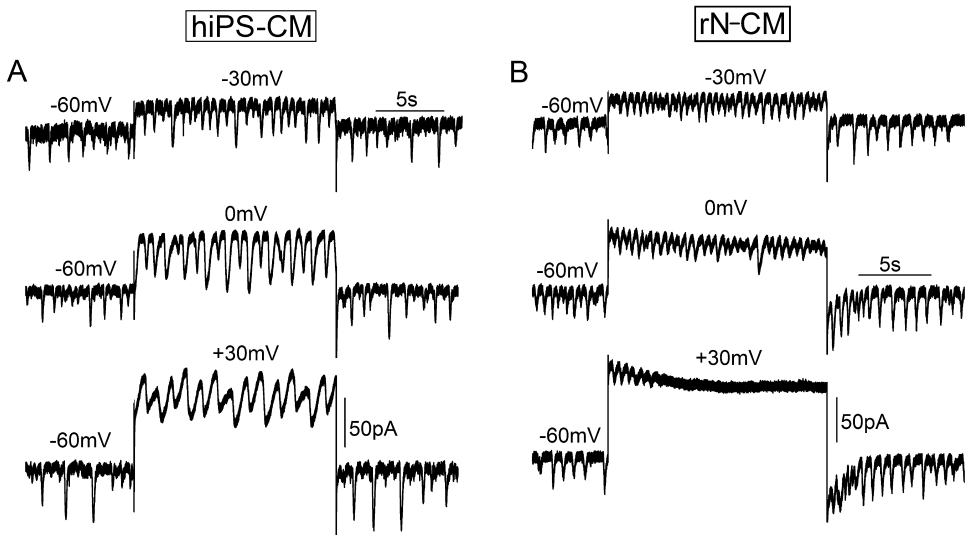

Fig. 3. Spontaneous beating of hiPS-CM (A) and rN-CM (B) are insensitive to changes in holding potential. Oscillations in I_{NCX} were insensitive to 15 s voltage-clamp depolarizations from −60 to −30 and 0 mV. Depolarization to +30 mV stopped oscillations of I_{NCX} in rN-CMs, but not in hiPS-CM. Capacitance: rN-CM 35 pF, hiPS-CM 36 pF. Cells were voltage-clamped at 35 °C and dialyzed with a solution containing 0.1 mM EGTA.

2.4. Voltage-clamp procedures

Cells were voltage-clamped in the whole-cell configuration at −50 or −60 mV to measure spontaneous oscillations in membrane current using a Dagan amplifier and pClamp software (Clampex 10.2). Action potentials were recorded in the current-clamp mode. Borosilicate patch pipettes were prepared using a horizontal pipette puller (Model P-87, Sutter Instruments, CA). The pipettes had a resistance of 3–5 MΩ. In most experiments the membrane under the patch pipette was ruptured and the cells dialyzed with Ca^{2+}-buffered pipette solutions containing (in mM): 110 Cs-aspartate, 15 NaCl, 20 TeaCl, 5 Mg-ATP, 0.1 EGTA with or without 0.05 or 0.1 Fluo-4, 0.1 $CaCl_2$ ($[Ca^{2+}]_i \cong 100$ nM), 10 glucose and 10 HEPES (titrated to pH 7.2 with CsOH). In some experiments the cells were examined with the perforated patch technique using pipette solutions containing (in mM): 145 Cs-glutamate, 9 NaCl, 1 $MgCl_2$, 10 HEPES (titrated to pH 7.2 with CsOH), and amphotericin B (Fisher Scientific) 0.69 mg/ml. The extracellular solution used during experiments contained (in mM): 137 NaCl, 5.4 KCl, 2 $CaCl_2$, 1 $MgCl_2$, 10 glucose and 10 HEPES (titrated to pH 7.4 with NaOH). Rapid applications of 3 mM caffeine and other compounds were used in the external K^+-free solutions to probe the cellular Ca^{2+} stores or spontaneous Ca^{2+} releases from SR. While most experiments were carried out at room temperature, 24 °C, some were performed at 35 °C as indicated in the legends.

2.5. Fluorometric Ca^{2+} measurements in voltage-clamped cells

Cytosolic Ca^{2+} $[Ca^{2+}]_i$, was measured routinely by including 0.1 mM Fluo-4 pentapotassium salt in the dialyzing pipette solution. Whole-cell fluorescence was measured using excitation with 460 nm light from an LED-based illuminator (Prismatix, Modiin Ilite, Israel) and detection of emitted light (>500 nm) with a photomultiplier tube that was placed behind a moveable, adjustable diaphragm, which served to limit the area of detection to the voltage-clamped cell. Fluo-4 loaded, voltage- or current-clamped cells were also imaged using rapid 2-D confocal microscopy (Odyssey XL, Noran Instruments, Middleton, WI) to chart the spread of spontaneous cytosolic Ca^{2+} transients (Figs. 4 and 5; [36]). The stacks of fluorescence images were collected at 30 or 120 Hz, using a 63× objective (Zeiss Plan-achromat, NA 1.4, oil) providing sampling on a 0.13 μm grid.

In other experiments we used adenoviral expression of genetically engineered Ca^{2+} probes. Cytosolic Ca^{2+} was measured in intact cells with a probe, GCamP6-FKBP that was targeted to ryanodine receptors with the FKBP-12.6 binding domain [27]. Mitochondrial Ca^{2+} signals were measured confocally with a novel mitycam probe, mitycam-E31Q [28] targeted to the mitochondrial matrix space at subunit VIII of human cytochrome c oxidase, contains mutant calmodulin with a relatively high K_d (~1.6 μM) for binding of Ca^{2+}, and uses yellow fluorescent protein as the reporting fluorophore. Unlike Fluo-4 and GCamP6-FKBP, mitycam-E31Q responds to increasing Ca^{2+} concentrations with a decrease in fluorescence.

2.6. Image processing

The collected stacks of fluorescence images showing spontaneous cytosolic and mitochondrial Ca^{2+} oscillations were low-pass filtered to display significant temporal and spatial variations. Individual frames were binned and filtered (2 × 2 or 3 × 3 pixel).

Cytosolic Ca^{2+} distributions measured with Fluo-4 were displayed ratiometrically (Figs. 4 and 5) as F/F_0 meaning $F(x,y,t)/<F_0(x,y)>$ where $F(x,y,t)$ is the low-pass filtered x-y image of a single frame measured at time t, and divisor is the baseline fluorescence image, $F_0 = <F_0(x,y)>$ which was calculated from several frames collected between beats. This point-by-point division was carried out only out to the edge of the cell where the fluorescence intensity fell below 10–15% of maximum. The ratiometric images were displayed at 30 Hz on a rainbow scale where the baseline ($F/F_0 \cong 1$) was shown in blue and elevated $[Ca^{2)+}]_i$ as warmer green, yellow, and red hues.

The mitochondrial Ca^{2+} distributions measured with mitycam-E31Q (Figs. 13 and 14) were displayed differentially as $\Delta F/F_0$ meaning $(F(x,y,t) - <F_0(x,y)>)/<F_0>$ where $<F_0>$ is a single number calculated as the average of $<F_0(x,y)>$ over the entire cell. Generally short sequences of differential images (4–8) were pooled to clearly show local variation in mitochondrial Ca^{2+} signaling.

The ratiometric images of cytosolic Ca^2 distributions and the differential images of mitochondrial Ca^{2+} signals formed the foundations for the identification of color-coded regions of interest (ROI) with distinct kinetics. The image analysis was carried out using a custom designed program, Con2i [36].

Please cite this article in press as: X.-H. Zhang, et al., Regionally diverse mitochondrial calcium signaling regulates spontaneous pacing in developing cardiomyocytes, Cell Calcium (2015), http://dx.doi.org/10.1016/j.ceca.2015.02.003

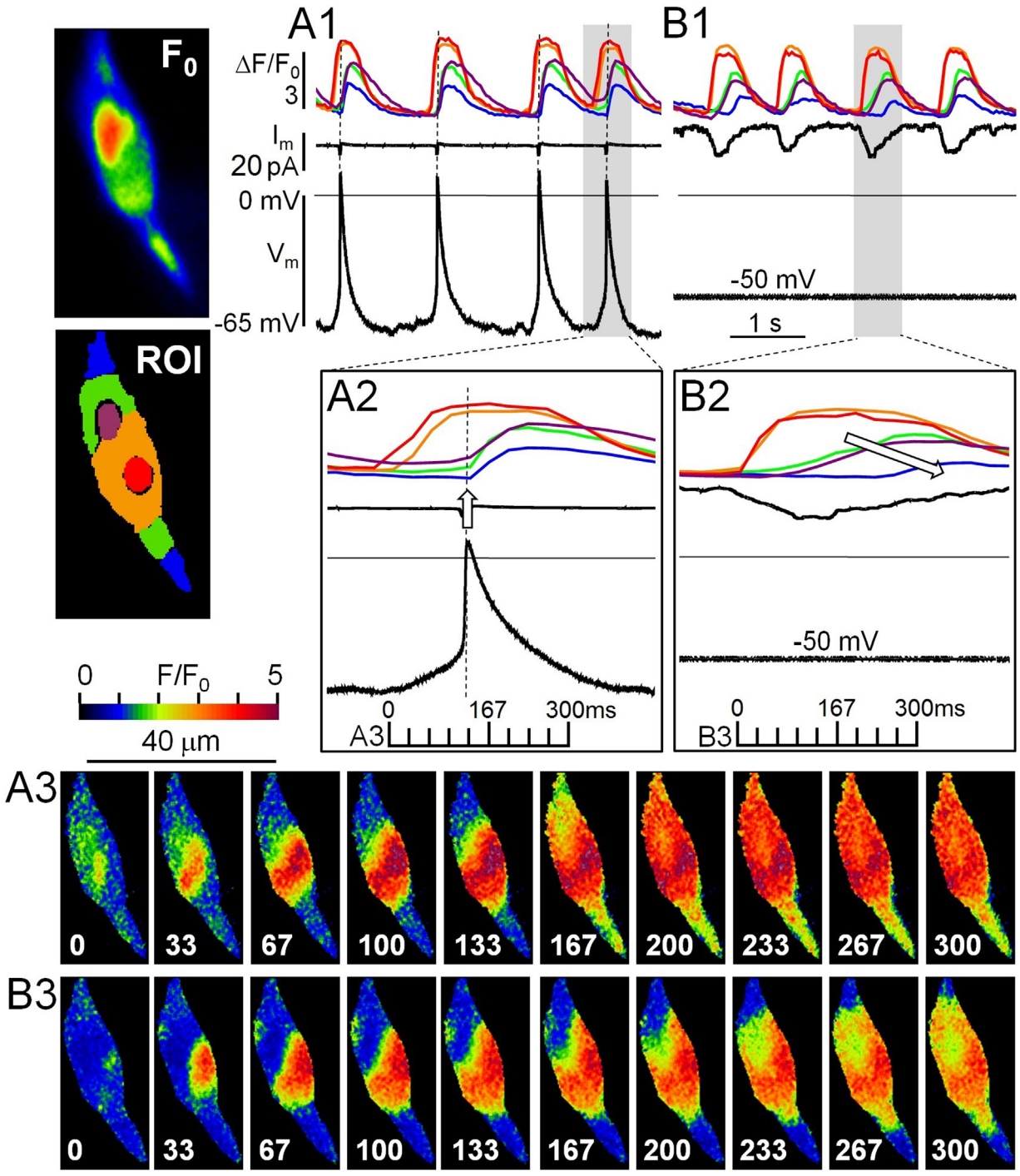

Fig. 4. The beating rates of a rN-CM are similar whether it generates action potentials under current-clamp control (A1, A2, A3) or Na^+-Ca^{2+} exchanger current is recorded at −50 mV holding potential (B1, B2, B3). (A1), (B1), (A2), (B2) Time course of color-coded regional Ca^{2+} signals ($\Delta F/F_0$), membrane current (I_m), and membrane potential (V_m). A3 and B3: Two sequences of 10 ratiometric fluorescence images measured at the times indicated in panels (A2) and (B2). F_0: Baseline fluorescence. ROI: Color-coded regions of interest (Red: approximate origin of spreading Ca^{2+} signals; purple: nucleus). Cells were voltage-clamped at 24 °C, and dialyzed with a solution containing 50 μM Fluo-4 to permit 2-D confocal imaging of cytosolic Ca^{2+} at 30 Hz.

2.7. Statistical analysis

Average values are presented in histograms and in the text as the mean ± the standard error of the mean for "n" cells. *T*-test was used to determine statistical significance. Significant findings are labeled with one ($p < 0.05$, *) or two stars ($p < 0.01$, **).

3. Results

3.1. Spontaneous beating: membrane current and Ca^{2+} transients

Fig. 1 illustrates simultaneous measurements at room temperature, 24 °C, of membrane current (I_{NCX}) and whole-cell cytosolic Ca^{2+} (Fluo-4) in hiPS-CM (A) and rN-CM (B) that were

Please cite this article in press as: X.-H. Zhang, et al., Regionally diverse mitochondrial calcium signaling regulates spontaneous pacing in developing cardiomyocytes, Cell Calcium (2015), http://dx.doi.org/10.1016/j.ceca.2015.02.003

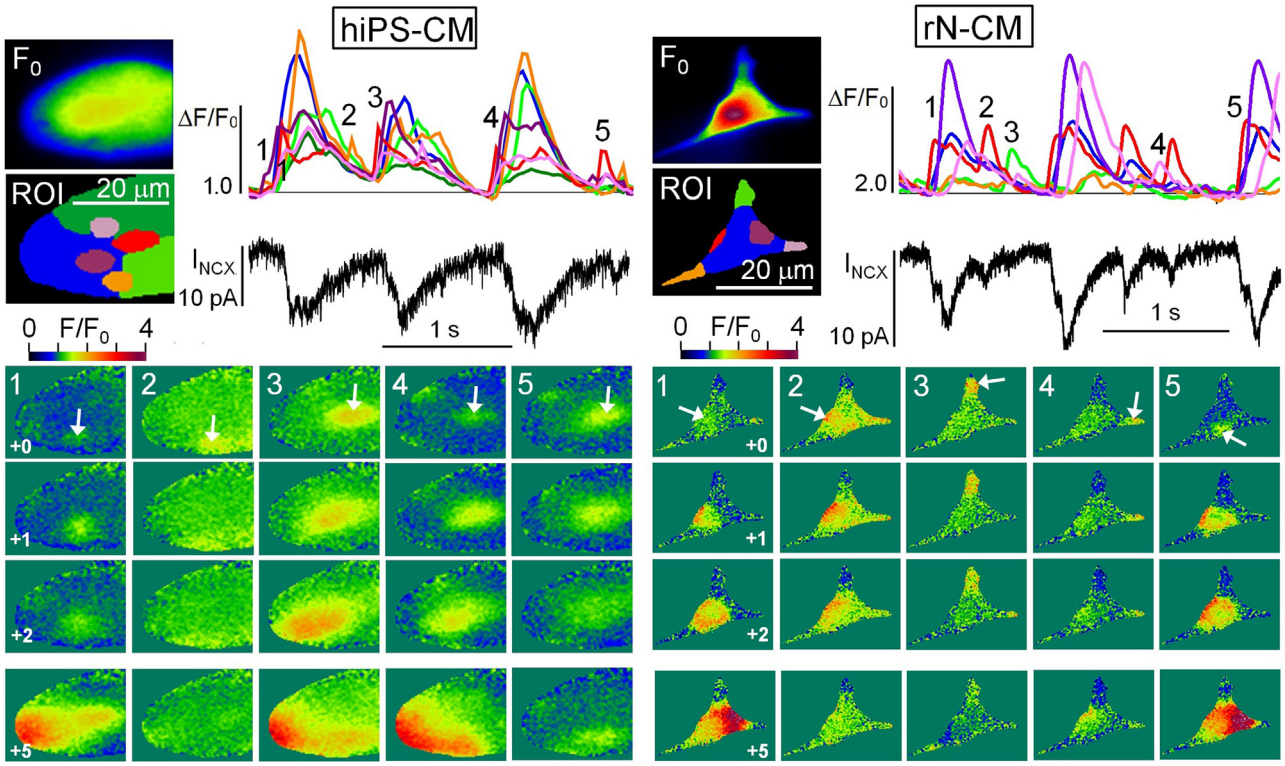

Fig. 5. Confocal images of spreading cytosolic Ca^{2+} oscillations in hiPS-CM (Movie_S2) and rN-CM (Movie_S3). The larger images in each panel show the baseline fluorescence (F_0) measured with dialyzed Fluo-4 and color-coded regions of interests (ROI) that were chosen to correspond to the shifting origins of Ca^{2+} waves and the larger expanses between them. The traces show the time course of the normalized fluorescence changes ($\Delta F/F_0$) in the ROIs and the simultaneously measured I_{NCX}. For each cell, the onset of each of 5 Ca^{2+} transients (1–5) is illustrated by 4 ratiometric images (+0, +1, +2, and +5) that were displayed at 30 Hz. The last (+5) was delayed 100 ms from the previous (+2) to show to what extend the Ca^{2+}-waves spread throughout the cell. As shown on the color scale, elevation of $[Ca^{2+}]_i$ is indicated by successive transitions from a greenish hue to yellow and red colors. Notice that some beats do not develop fully (rN-CM: 2, 3 and 4; hiPS-CM: 2 and 5) and that this is associated with reduced I_{NCX} and shifting sites of origination of the Ca^{2+} waves. Cells were voltage-clamped at 24 °C at a holding potential of −50 mV, dialyzed with a solution containing 0.1 mM Fluo-4, and imaged confocally at 120 Hz.

voltage-clamped at −50 mV, dialyzed with an internal solution containing 100 μM Fluo-4. Both cell types produced rhythmic Ca^{2+} oscillations that activated in-phase transient inward currents that were attributed to the Na^+-Ca^{2+} exchanger since they occurred in the absence of membrane potential excursions and had nearly the same time course as the measured Ca^{2+} transients. Interruption of spontaneous rhythmic activity by rapid application of caffeine also generated transient rises in global Ca^{2+} that were accompanied by large transient inward I_{NCX} and transiently blocked pacing suggesting involvement of SR Ca^{2+} stores. Quantification of the beating frequency and the amplitude of caffeine-induced I_{NCX} in rN-CM and hiPS-CM, suggested somewhat higher beating rates in rN-CM (Fig. 1C), but larger density of I_{NCX} in hiPS-CM (Fig. 1D).

The spontaneous beating continued uninterrupted under broad array of experimental conditions. The visible contractions that guided the selections of cells had the same frequency as the Ca^{2+}- and I_{NCX} -signals that generally continued for minutes after establishing the whole-cell voltage-clamp configuration. Recordings from rN-CM in the perforated-patch configuration and without Ca^{2+}-dyes showed faster pacing when the temperature was raised to 35 °C, but the frequency was the same whether the cells generated I_{NCX} transients at a holding potential of −50 mV or generated action potentials in the current-clamp mode (Fig. 2A and B). This was also the case when genetically engineered Ca^{2+} probes (Fig. 2C) were used as indicators of beating, and it was observed under current-clamp conditions that the Ca^{2+}-transients started to develop prior to the upstroke of the action potential (Fig. 2D and E). Similar action potentials were recorded in hiPS-CM in the current-clamp mode.

To examine the effects of membrane potential more fully we performed voltage-clamp experiments, with membrane rupture and cell dialysis, on hiPS-CM and rN-CM where the beating was assessed by measuring oscillations in the exchanger current, I_{NCX}, during clamp pulses lasting 15 s. In both cell types the beating rate was insensitive to potentials ranging from −60 to 0 mV, but often slowed or stopped at more positive voltages (Fig. 3). Spontaneous membrane current oscillations also continued to occur at hyperpolarizing potentials between −60 and −90 mV, but the frequency of the oscillation decreased somewhat as their magnitudes became larger and longer (data not shown).

To analyze these robust and persistent I_{NCX} and Ca^{2+} oscillations we performed 2-D confocal fluorescence microscopy at 30 or 120 Hz of voltage-clamped cell that were dialyzed with 50 μM Fluo-4. Again we found that spontaneous Ca^{2+} transients ($\Delta F/F_0$) occurred with similar frequency whether the cell generated action potentials (V_m) with maximal diastolic potentials of ∼−65 mV (Fig. 4A1), or generated inward I_{NCX} current at −50 mV (B1). Detailed examination, on an expanded time scale, revealed that the diastolic depolarization period coincided with local increases in Ca^{2+}, which became endemic once the action potential was triggered (Fig. 4A2, ↑).

The spreading Ca^{2+} signals could be followed in sequential ratiometric confocal images (Fig. 4A3 and B3) and the time-course of the normalized fluorescence intensities (corresponding to selected color-coded regions of interest, ROI; Fig. 4A2 and B2). At 30 Hz imaging speeds, both action potential- and voltage-clamp-activated image sequences show emergence of a local Ca^{2+} signal near the center of the cell (Frame 0, red ROI)

Please cite this article in press as: X.-H. Zhang, et al., Regionally diverse mitochondrial calcium signaling regulates spontaneous pacing in developing cardiomyocytes, Cell Calcium (2015), http://dx.doi.org/10.1016/j.ceca.2015.02.003

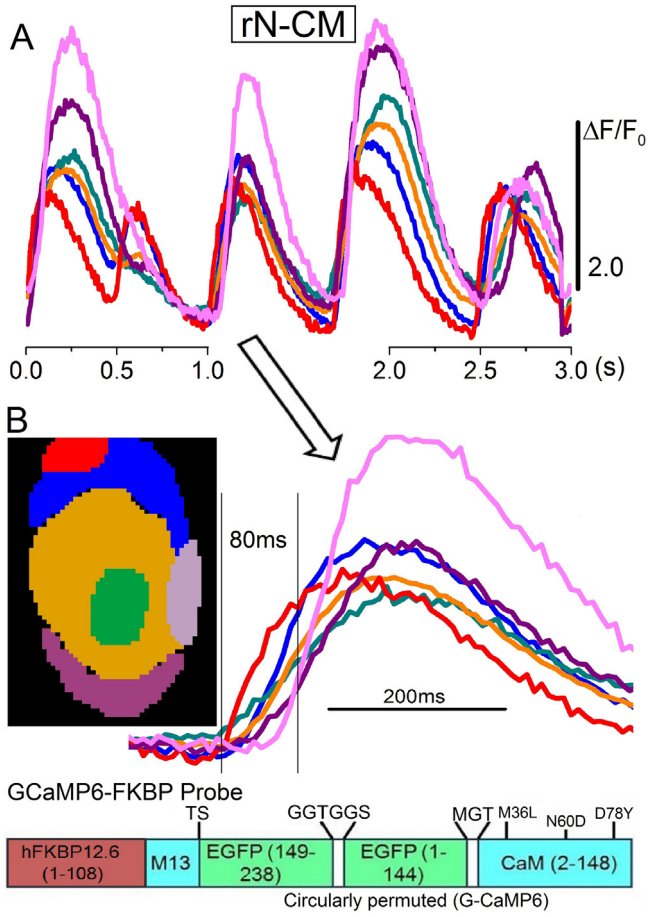

Fig. 6. Spontaneous Ca^{2+} signals in an intact, non-voltage clamped rN-CM expressing GCamP6-FKBP probe. (A) Spreading cytosolic Ca^{2+} signals recorded confocally at 120 Hz. The curves show the time course of the fluorescence changes in selected ROIs. The same records are illustrated in Movie_S1. (B) Color-coded regions of interest (left) and second beat on an expanded time scale (right). The diagram at the bottom shows the design of the expressed Ca^{2+}-sensing probe GCamP6-FKBP.

and similar spreading of Ca^{2+} waves in the adjoining orange-colored ROI in the following 4 frames (33, 67, 100 and 133 ms). Perhaps more significantly, under current-clamp conditions, large rises in cytosolic Ca^{2+} appear to take place (red ROI) during the slow diastolic depolarization period, prior to triggering of action potential and further rapid rise of Ca^{2+} that spreads to the ends of the cell (Fig. 4A3, frame 167 ms). Under voltage-clamp condition, however, the Ca^{2+} wave, in the same cell, continues to spread slowly and with decreasing amplitudes (Fig. 4B2, 4 o'clock arrow) and appears not to invade the ends of the cell by 300 ms (Fig. 4B3, frame 300 ms, blue ROI). Consistent with this pattern, most voltage-clamped, and dialyzed hiPS-CM and rN-CM generated Ca^{2+} waves that typically originated from a relatively fixed central, peri-nuclear location, spread to the entire cell and were accompanied by significant activation of I_{NCX} (10-30 pA, but occasionally generated smaller Ca^{2+} signals that remained localized and generated little or no detectable I_{NCX} (Fig. 5). Using less invasive procedures, we used GCamP6-FKBP to measure Ca^{2+} signals in spontaneously beating, intact, non-dialyzed, non-patched cells and found persistent Ca^{2+} oscillations where synchronous rises in Ca^{2+} most likely reflect generation of action potentials, while the localized or slowly spreading Ca^{2+} signals resulted from failure to reach the thresholds for electrical excitation (Fig. 6).

Since pacing at distinct frequencies was robustly present in both rN-CM and hiPS-CM irrespective of methodology used (perforated-patch *vs.* cell dialysis *vs.* intact cells; dim light for whole-cell measurements *vs.* strong light for confocal imaging, 24 *vs.* 35 °C, voltage- *vs.* current-clamp and Fluo-4 *vs.* GCamP6-FKBP as Ca^{2+} probe), in the next set of experiments we focused on Ca^{2+}- and voltage-dependence of spontaneous pacing by: (a) using holding potential of −50 mV to prevent activation of voltage-gated ion channels; (b) dialyzing with 0.1 mM Fluo-4 to allow detailed and fast Ca^{2+} measurements and (c) experimenting at 24 °C (instead of 35 °C) to slow pacing frequency in order to more clearly monitor the sequence of events during the diastolic interval. With this general approach we assessed beating by measuring membrane current, I_{NCX}, and cytosolic Ca^{2+} transients where contractions were suppressed by blebbistatin [29].

3.2. Hyperpolarization-activated current, I_f, and spontaneous beating

Since spontaneous beating activity in the SA-nodal cells has been associated with the hyperpolarization-activated cyclic nucleotide-gated current, I_f, we examined the possible activation of this channel during spontaneous beating activity. We found significant expression of I_f channel in hiPS-CM, but not in spontaneously pacing rN-CM. Fig. 7A and B quantify the current density of I_f in hiPS-CM at different voltages and compares them to those recorded in mouse iPS-CM (miPS-CM) and rN-CM. It is clear that there was little or no significant activation of I_f at voltages positive to −80 mV in either miPS-CM and hiPS-CM and none in rN-CM at any hyperpolarizing voltage. Furthermore, the small amounts of I_f activated at −80 or −90 mV had activation kinetics that were too slow (seconds) to contribute significantly to rapid spontaneous beating (~2 s^{-1}). Fig. 7D, confirms that 2 mM Cs^+, reported to block I_f in SA-nodal cells [37], rapidly and reversibly blocked I_f, in hiPS-CM. Thus neither the voltage-dependence and kinetics, nor the pharmacology of I_f channels is consistent with its contribution to the spontaneous beating activity of rN-CM or mouse iPS-CM. Consistent with this idea, 10 μM ivabradine, a potent and specific blocker of I_f in SA-nodal cells [38] had no effect on spontaneous beating frequency or on the current oscillations activated at −50 mV in hiPS-CM or rN-CM (Fig. 7E and F).

3.3. Ca^{2+} current and spontaneous beating

Since L-type Ca^{2+} channels are critically important in regulation of pacemaking activity in SA-nodal cells [37,39], and in the light of recent reports that nifedipine suppresses spontaneous beating in hiPS-CM [40,41], we measured the effectiveness of nifedipine in suppressing the spontaneous Ca^{2+} transient and membrane current oscillations recorded at −50 mV. We found that 5–10 μM nifedipine while fully suppressing I_{Ca} decreased the rate of spontaneous oscillation and their amplitude by only ~20% in hiPS-CM or rN-CM (Fig. 8A and C) after ~1 min. Under these conditions, significant rise in cytosolic Ca^{2+}, though with slower kinetics, was activated with depolarizing pulses to 0 mV in the I_{Ca}-suppressed cells (Fig. 8B and D; upper traces), suggesting significant influx of Ca^{2+} on NCX and/or its release from the SR, independent of I_{Ca}-triggered release, underlies the spontaneous beating of these developing cardiomyocytes. Longer exposures (>~5 min) of nifedipine were accompanied by irreversible loss of I_{Ca} and irregular beating suggesting run-down or slow changes in the Ca^{2+} balance of the voltage clamped cells.

3.4. Na^+-Ca^{2+} exchanger and spontaneous beating

To identify the molecular entity responsible for generation of spontaneous rhythmic oscillations in the membrane current in these minimally Ca^{2+}-buffered (0.1 mM EGTA or Fluo-4 plus 0.1 mM

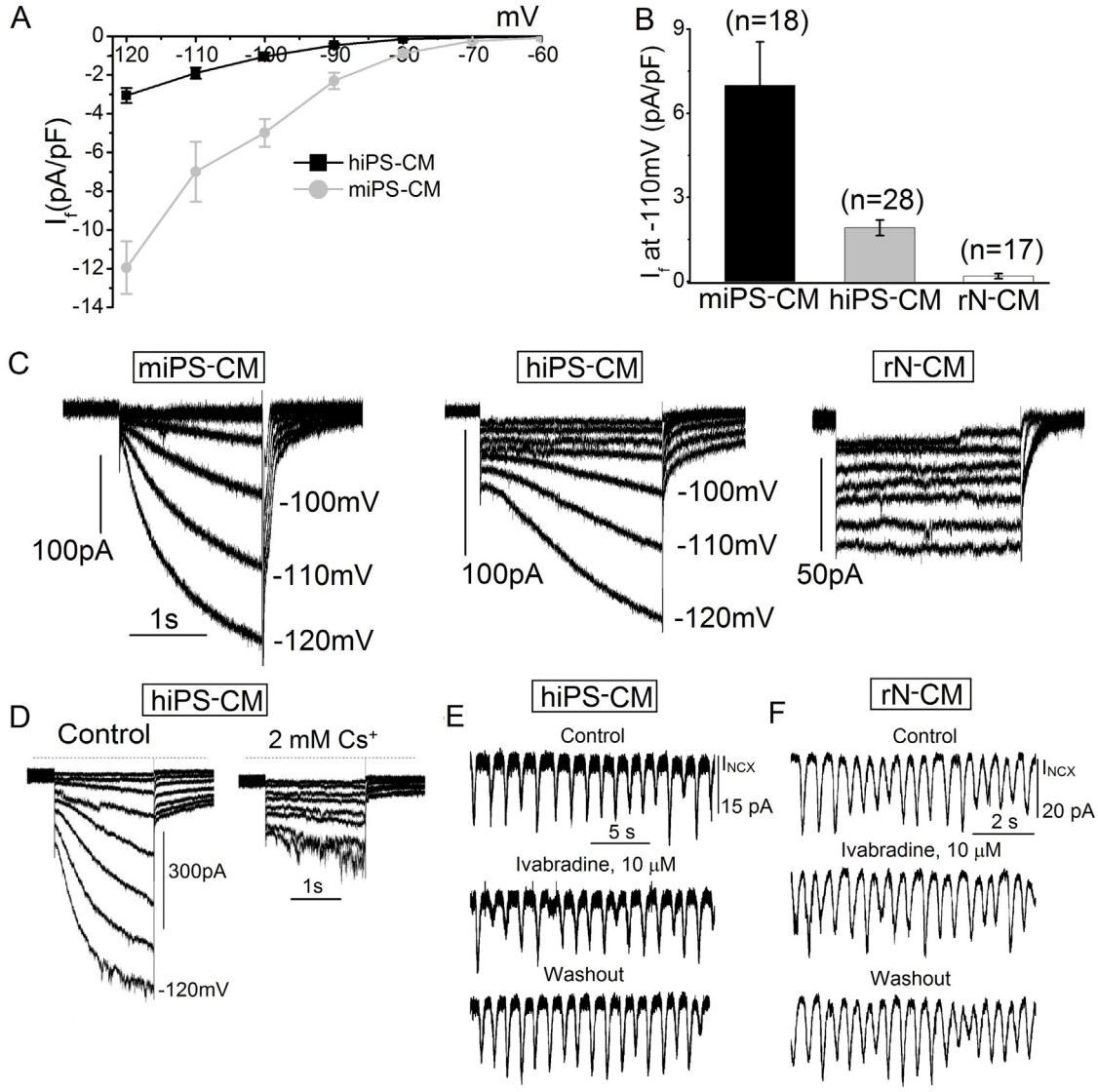

Fig. 7. I_f and its lack of effect on pacing at fixed membrane potential. (A) Voltage-dependence of I_f in mouse (miPS-CM) and human (hiPS-CM) stem cell-derived cardiomyocytes. (B) Average I_f at −110 mV is larger in mouse than in hiPS-CM, and is virtually absent in rN-CM. (C) Sample traces of membrane current in the three cell types during 2.5 s hyperpolarizations from −40 mV to potentials from −60 to −120 mV. (D) Sample recordings with the same protocol in hPS-CM showing block of I_f by 2 mM Cs^+. (E) and (F) Addition of 10 μM ivabradine to suppress I_f had no effect on oscillations of I_{NCX} in hiPS-CM (E) or rN-CM (F). The cells were voltage-clamped at 24 °C and dialyzed with a solution containing 100 μM EGTA.

Ca^{2+}) cells, we tested the sensitivity of this current to NCX-blockers KB-R7943 (10 μM), Ni^{2+} (5 mM) and Cd^{2+} (2 mM). KB-R7943 had little immediate effect (Fig. 9A and D), but in 15-30 s it decreased by 60–80% (histograms) the magnitude of spontaneously occurring transient inward currents and the currents activated by caffeine-triggered Ca^{2+}-release in both hiPS-CM and rN-CM (Fig. 9A and D). In voltage-clamped cells dialyzed with Fluo-4, we found that the greatly attenuated spontaneous oscillations of I_{NCX} that still persisted in the presence of KB-R7943 (*s in Fig. 9A and D) were accompanied by cytosolic Ca^{2+} transients that were often somewhat irregular in frequency, but of near normal amplitude (Fig. 9B and E). To achieve a faster and more complete and reversible block of I_{NCX}, we used Ni^{2+} (5 mM) or Cd^{2+} (2 mM). Under voltage-clamp conditions, Ni^{2+} effectively blocked I_{NCX}, but left strong spontaneous and caffeine-induced Ca^{2+} signals that, as expected, showed marked suppression of rate of relaxation (Fig. 9C; *Cf.* [42]). Similarly, spontaneously developing Ca^{2+} signals continued unabated when rapid application of Cd^{2+} blocked the generation of action potentials in cells that were current-clamped at 35 °C in the perforated patch configuration (Fig. 9F). It is plausible that longer lasting exposures to KB-R7943 may block both sarcolemmal and mitochondrial Na^+-Ca^{2+} exchangers while divalent cations under current-clamp conditions may block the action potentials by blocking voltage-gated ion channels. Collectively the results illustrated in Fig. 9 suggest that rapid block of I_{NCX} does not abolish spontaneous Ca^{2+} oscillations in hiPS-CM and rN-CM.

3.5. I_{Ca}-gated Ca^{2+} release from the SR and spontaneous beating

To probe the role of SR in the generation of spontaneous beating, we used agents that either blocked RyRs or depleted the SR Ca^{2+} content. We found that application of 100–200 μM tetracaine, known to suppress SR Ca^{2+} release [43], arrested spontaneous beating rapidly and reversibly in both cell types clamped at −50 mV (Fig. 10A and C). Using longer exposures to tetracaine, spontaneous beating often recovered and was accompanied by sporadic

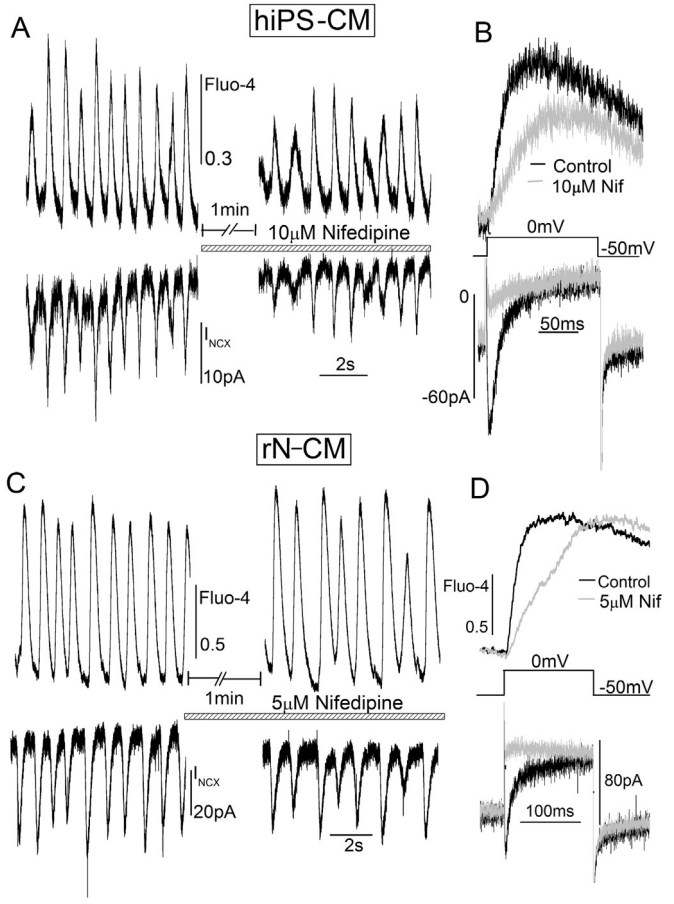

Fig. 8. The Ca^{2+} channel blocker nifedipine blocks I_{Ca} (B and D), but has only a minor effect on spontaneous oscillations of I_{NCX} and $[Ca^{2+}]_i$ (A and C) in hiPS-CM (A and B; 10 μM, $n = 3$) or rN-CM (C and D; 5 μM, $n = 3$). Panel (B) and (D) show that 5 or 10 μM nifedipine effectively blocked I_{Ca} activated by depolarization to 0 mV (lower traces) and delayed the development of Ca^{2+}-dependent fluorescence (upper traces). Cells were voltage-clamped at 24 °C using a holding potential of −50 mV and dialyzed with a solution containing 0.1 mM Fluo-4, which was excited with low intensity 460 nm light for cytosolic whole-cell Ca^{2+} measurements.

larger releases of Ca^{2+} (Fig. 10 B). The first beat after washout of tetracaine was often accompanied by larger Ca^{2+} release and I_{NCX}, reflecting increased SR Ca^{2+} content during tetracaine block of RyRs (e. g. Fig. 10A).

Thapsigargin, a widely used inhibitor of Ca^{2+}-ATPase in mammalian cells, suppressed the spontaneously activating I_{NCX} in 3–5 min and caffeine triggered I_{NCX} in 5–7 min in rN-CM, when used in a concentration of 5 μM (Fig. 11E–H). The effects developed more slowly with 0.5 μM thapsigargin in hiPS-CMs (Fig. 11A–D). Thus both sets of data support the idea that Ca^{2+} release from the SR plays a critical role in supporting spontaneous beating in the developing cells.

3.6. Mitochondrial un-coupler FCCP arrests spontaneous pacing

Since mitochondria constitute ~30% of the myocyte volume [44] and a number of reports suggest a critical role for mitochondria in cardiac Ca^{2+} signaling [18,45], we probed the extent to which mitochondria regulate spontaneous beating. Using short exposures to low concentrations of FCCP (50–100 nM), we found that this mitochondrial uncoupler abolished I_{NCX} and Ca^{2+} transients associated with spontaneous pacing (Fig. 12A1 and B1). The suppressive effect of FCCP was accompanied by significant slowing in the rates of relaxation of the caffeine-induced I_{NCX} and Ca^{2+} transients (Fig. 12A2 and B2), but amplitudes remained nearly intact (Fig. 12A3 and B3), suggesting that SR Ca^{2+} loads and NCX activities were not affected substantially by FCCP in the low concentrations of drug used. These low concentrations of FCCP are reported to enhance oxidative mitochondrial metabolism without depolarizing the mitochondria [30] and were fully reversible after 2–3 min of drug washout.

We also tested directly whether I_{NCX} might be suppressed by FCCP by using depolarizing/repolarizing ramp pulse protocols, from −60 to +80 mV and back to −100 mV, to measure both the influx and efflux of Ca^{2+} on NCX. Fig. 12C shows that 100 nM FCCP had no significant effect on I_{NCX} measured at −100 and +80 mV even though it suppressed I_{Ca} as seen during the ramp-clamps at potentials between −30 and +60 mV. This finding was further supported by the results where influx of Ca^{2+} on NCX was measured using the Na^+ withdrawal procedure. Fig. 12D and E shows that the outward I_{NCX} activated on rapid withdrawal of Na^+ (red and black traces) were not significantly affected by exposure to 50 nM FCCP in either hiPS-CM or rN-CM (histograms). The prolongation of relaxation time of caffeine-induced Ca^{2+} transients, and suppression of spontaneous pacing by short exposures of FCCP (Fig. 12A and B), suggests a direct role for mitochondria in the cycling of cytosolic Ca^{2+} and regulation of pacing.

3.7. Measurements of mitochondrial Ca^{2+} in mitycam-E31Q infected cells

In spontaneously beating hiPS-CM or rN-CM, infected for 2–3 days with a genetically encoded mitochondrial Ca^{2+}-sensing probe, mitycam-E31Q [28], we measured oscillations in the global mitycam signals that accompanied membrane current oscillations. Such global signals were, however, small in amplitude, and varied in kinetics as also reported earlier for adult myocytes [46]. To examine whether regional heterogeneity in mitochondrial populations contributes to the variability of global mitycam signals, we used confocal microscopy to identify regions of interest (ROI) with different Ca^{2+}-signaling profiles and analyzed the results along the same lines used for imaging of cytosolic Ca^{2+} with Fluo-4. Fig. 13 illustrates how this approach was used to analyze the patterns of mitochondrial Ca^{2+} signals in hiPS-CM and rN-CM in control conditions and where spontaneous beating was suppressed by 30 s exposures to 50 nM FCCP. The images of baseline fluorescence (F_0) showed that the mitycam-E31Q probe, targeted to mitochondrial subunit VIII of human cytochrome C, clustered around the nuclei of the cells (n). Under control conditions, as spontaneous beating activated large I_{NCX} transients (Figs. 1, 3, 5 and 7–13), the mitochondrial probe signal unexpectedly showed regionally diverse patterns, such that while some mitochondrial populations showed decrease in fluorescence (uptake of Ca^{2+}), others displayed an increase in fluorescence corresponding to Ca^{2+} release. The mitochondrial populations showing Ca^{2+} release signals were essentially conserved in hiPS-CM (Fig. 13A1 and A2, red trace and ROI) and rN-CM (Fig. 13B1 and B2, red and orange traces and ROIs) from one beat to the next, consistent with findings of dominant pacing sites (Figs. 4–6). The release sites were generally surrounded by mitochondria that appeared to concurrently take up Ca^{2+} (Fig. 13, green, blue, purple ROI in hiPS-CM; primarily blue ROI in rN-CM). Addition of FCCP suppressed the dominant pacing site and regular spontaneous beating, but left greatly reduced and discordantly activating I_{NCX} that were associated with more locally confined oscillatory mitochondrial Ca^{2+} signals where Ca^{2+} releases and uptakes were seen to switch back and forth between neighboring ROIs. For instance, as seen in the illustrated hiPS-CM (Fig. 13A1), the release was seen to switch from the purple ROI to the red and back again. These patterns of mitochondrial Ca^{2+} signaling are characteristic of 4 recordings in rN-CM and 3 recordings in hiPS-CM and are consistent with the

Please cite this article in press as: X.-H. Zhang, et al., Regionally diverse mitochondrial calcium signaling regulates spontaneous pacing in developing cardiomyocytes, Cell Calcium (2015), http://dx.doi.org/10.1016/j.ceca.2015.02.003

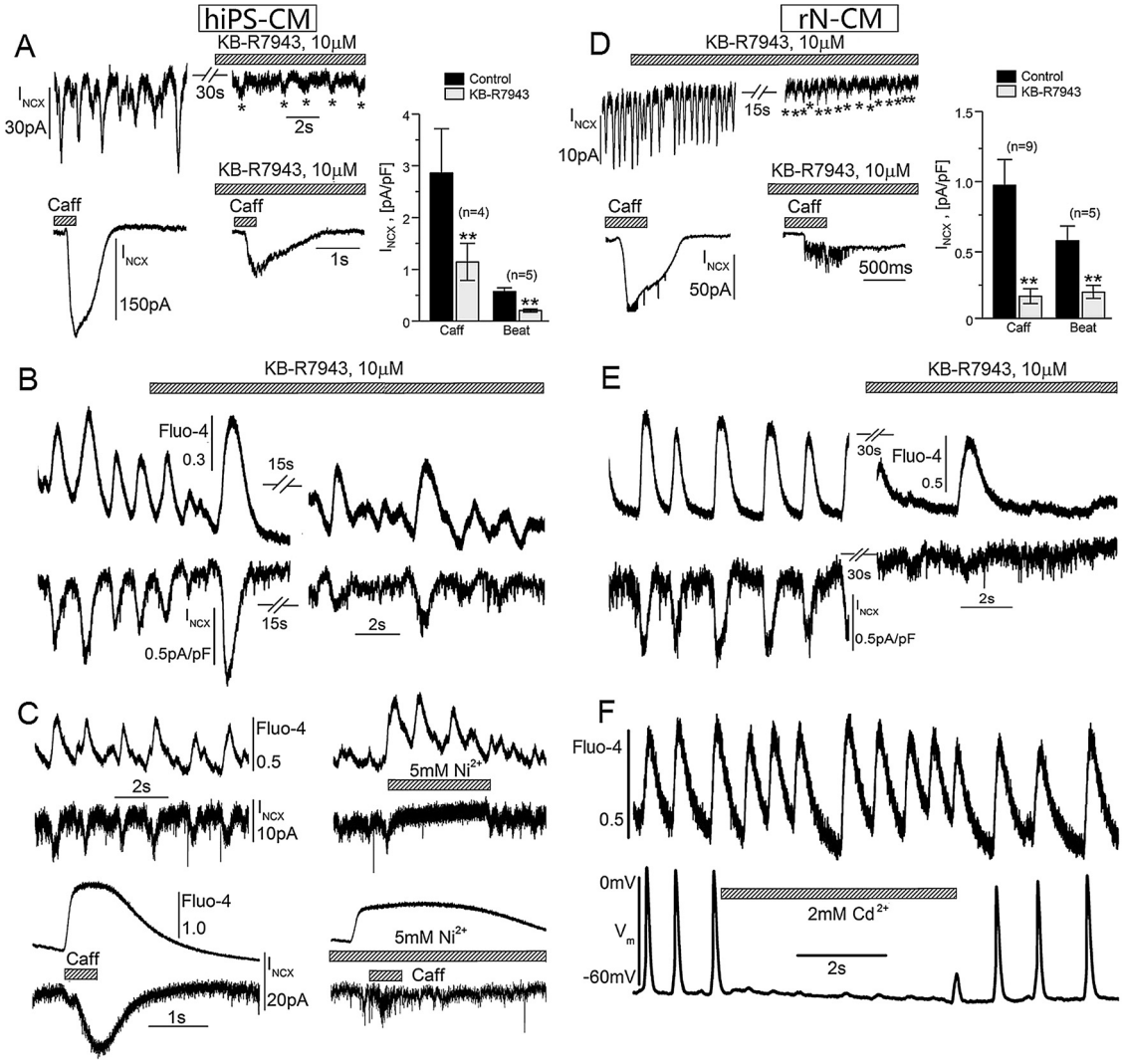

Fig. 9. KB-R7943 (A, B, D, E, 10 μM), Ni^{2+} (C, 5 mM), and Cd^{2+} (F) suppress I_{NCX} in hiPS-CM (A)–(C) and rN-CM (D)–(F), but do not abolish spontaneous Ca^{2+} oscillation or caffeine-induced Ca^{2+} release. (A) and (D) Exposures to KB-R7943 for 15-30 s suppress spontaneously oscillating (upper panels) and caffeine-induced I_{NCX} (lower panels) only by 60–80% (histograms) thereby leaving indications of continued Ca^{2+} oscillations (*). (B) and (E) Simultaneous measurements with Fluo-4 confirm the continuation of spontaneous cytosolic Ca^{2+} oscillations when I_{NCX} is suppressed by KB-R7943. (C) Rapid exposure of hiPS-CM to 5 mM Ni^{2+} blocks I_{NCX} while accentuating associated spontaneous $[Ca^{2+}]_i$ oscillations (top) and prolonging the duration of caffeine-induced $[Ca^{2+}]_i$ transients (bottom). (F) Rapid exposure of a current-clamped rN-CM reversibly blocked action potentials without affecting cytosolic Ca^{2+} oscillations measured with GCamp6-FKBP (*Cf.* Fig. 6). The cells were voltage-clamped at 24 °C (A)–(E) using dialyzing solutions containing 100 μM EGTA (A) and (D) or Fluo-4 (B), (C), (E) or current-clamped in the perforated patch configuration at 35 °C (F).

Fluo-4 measurements of cytosolic Ca^{2+} (Fig. 12A and B) suggesting that mitochondria play an active role in Ca^{2+}-mediated pacing in these developing cells.

Releases and uptakes of Ca^{2+} by distinct mitochondrial populations were also observed in both hiPS-CM and rN-CM in response to rapid puffs of 3 mM caffeine that also activated large I_{NCX} (Fig. 14). As anticipated from Fig. 12, short (30–60 s) exposures to 50 nM FCCP significantly slowed the decay of I_{NCX} (Fig. 14A1 and B1, lower traces), but produced only minor reduction in its magnitude (Fig. 14 A3 and B3, right histograms). Simultaneously measured mitochondrial Ca^{2+} signals were similarly prolonged (Fig. 14A1 and B1, upper traces) while their amplitudes corresponding to both uptake and release were reduced relatively little initially (Fig. 14A3 and B3, left histograms). Similarly, baseline mitycam fluorescence after addition of FCCP was 80 ± 3% (rN-CM, $n = 6$) or 83 ± 7% (hiPS-CM, $n = 6$) percent of control, indicating that the mitochondrial Ca^{2+} content remained largely intact. The effects of exposure to 50–100 nM FCCP for 1–3 min were fully reversible. When used in higher concentrations (1 μM), FCCP irreversibly damaged mitochondrial Ca^{2+} handling.

4. Discussion

The quintessential property of developing cardiomyocytes is their ability to beat rhythmically in culture, a property also observed in early stages of embryonic development, long before the heart evolves its multi-chambered structure. Here, we have attempted to probe the mechanisms underlying the spontaneous rhythmic beating of cardiomyocytes in two cell models: (1) Neonatal rat cardiomyocytes isolated from 1–6 day old rat hearts, and (2) spontaneously beating human iPS cell-derived cardiomyocytes [25]. Because we have already reported that Ca^{2+}-signaling properties of rN-CM and hiPS-CM were similar to those of freshly isolated adult cardiomyocytes [26,31], our approach was to image focal changes in Ca^{2+} profiles in spontaneously beating cells either dialyzed with Fluo-4 or infected with genetically encoded Ca^{2+} probes

Please cite this article in press as: X.-H. Zhang, et al., Regionally diverse mitochondrial calcium signaling regulates spontaneous pacing in developing cardiomyocytes, Cell Calcium (2015), http://dx.doi.org/10.1016/j.ceca.2015.02.003

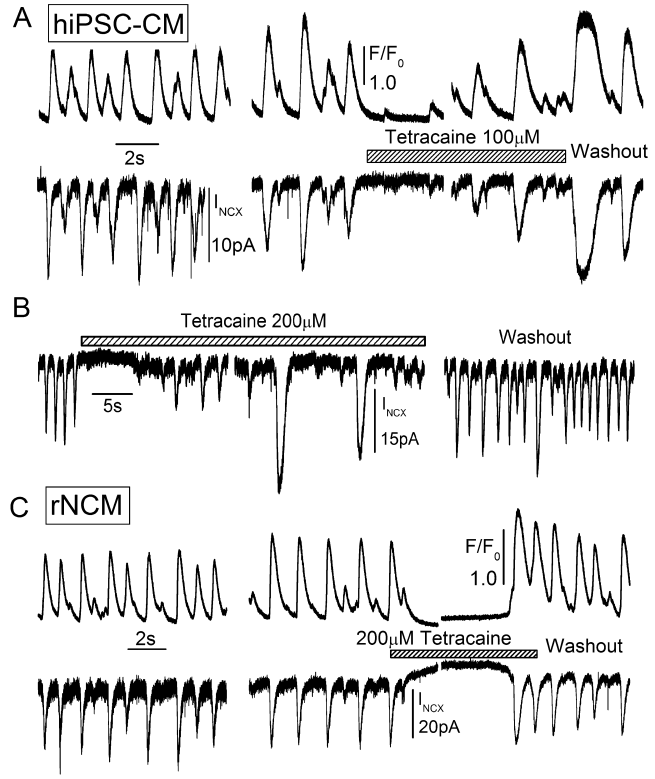

Fig. 10. Transient suppression of spontaneous oscillations of Ca^{2+}-dependent fluorescence (F/F_0) and I_{NCX} in voltage-clamped hiPS-CM (A and B) and rN-CM (C) by the ryanodine receptor-blocker tetracaine (100 or 200 μM) during short-term (A and C) and long-term (B) exposure. The first beat after washout of tetracaine was generally larger, indicative of an increased SR Ca^{2+} load during tetracaine exposure. In some cells, during the tetracaine exposure and cessation of spontaneous activity, sporadic but large transient inward currents were activated (B), that were thought to be related to unblocking of tetracaine-block as the Ca^{2+} load of SR increases in the presence of the drug (A). Similar data were also obtained in rN-CM. Cells were voltage-clamped at 24 °C at a holding potential of −50 mV, and dialyzed with a solution containing 0.1 mM Fluo-4, which was excited with low intensity 460 nm light for whole-cell measurements of cytosolic Ca^{2+}.

directed at ryanodine receptors (GCamP6-FKBP) or mitochondria (mitycam-E31Q [28]). Fluo-4 confocal imaging showed that while Ca^{2+} signaling started at a preferred central location and spread throughout the cell in a repeatable pattern, the mitycam E31Q mitochondrial probe showed divergent patterns of Ca^{2+} release and uptake during spontaneous pacing. The finding that spontaneous pacing rate in developing myocytes were not significantly affected by triggering of action potential, but was highly sensitive to low concentrations of mitochondrial un-coupler FCCP, suggests that the primary pacing mechanism may be independent of activation of ion channels, but highly dependent on metabolic state of mitochondria.

4.1. Expression of hyperpolarization-activated current, I_f, and spontaneous rhythmic beating

Fig. 7 suggests significant differences in the level of expression of I_f in rN-CM and human or mouse iPS-CM. Interestingly, even though rat neonates do not express I_f (Fig. 7B–C), the frequency of its spontaneous beating was significantly higher than that of human iPS-CM (Fig. 1). Expression of I_f in iPS-CM was more robust and was present in every cell examined, but I_f activated only at potentials negative to −80 mV in human and −70 mV in mouse iPS-CM, and was rapidly and reversibly blocked by 2 mM Cs^+ (Fig. 7D) without significantly altering the pacing frequency, as reported also for human and rabbit SA-nodal cells [47,48]. Thus, if I_f were to contribute to generation of spontaneous activity, it would have to carry significant inward current at voltages positive to −70 mV, clearly not the case here, where I_f is either absent or its kinetics too slow and activation-voltage too negative. Furthermore, the pacing rate was unaltered by blockers of I_f (Fig. 7E and F), changes in holding potential (Fig. 3, −60 to 0 mV), and the triggering of action potentials (Figs. 2, 4 and 9). Pacing frequency did not vary significantly between intact non-dialyzed cells (Fig. 6), and cells voltage-clamped at −50 mV, but the frequency accelerated significantly (to ∼3/s in rN-CM) when the temperature was increased from 24 to 35 °C under perforated patch conditions (Fig. 2). Thus, our findings argue for a mechanism independent of membrane ion channels initiating the spontaneous rhythmic beating.

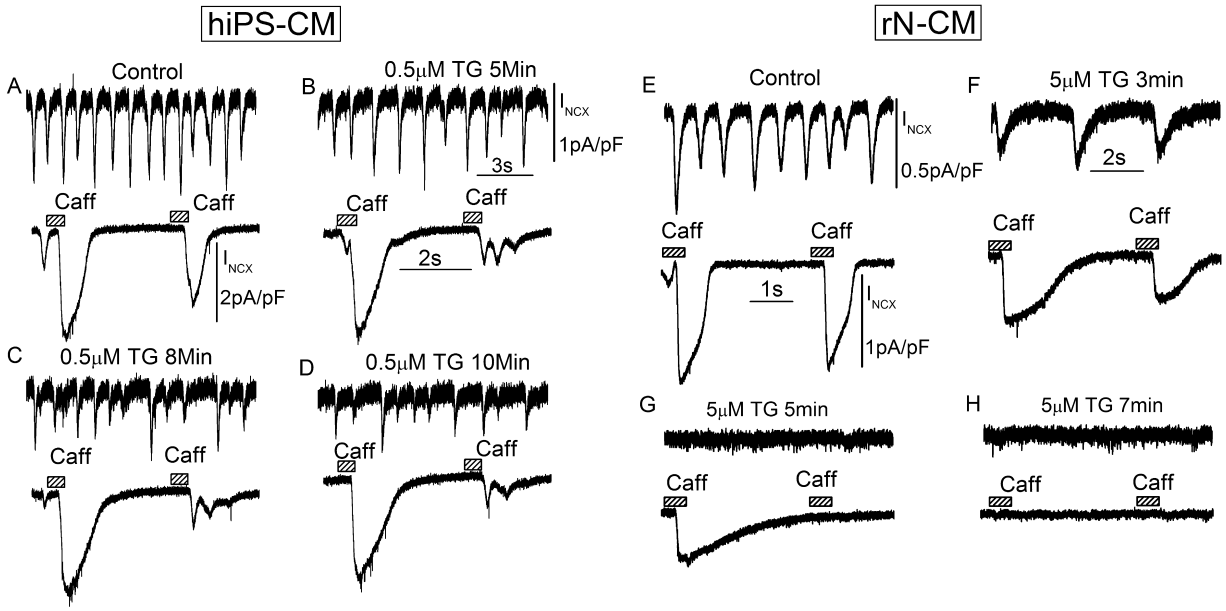

Fig. 11. Effect of thapsigargin, an inhibitor of Ca^{2+}-ATPases (SERCA2a) on membrane current, I_{NCX}, in hiPS-CM (A–D) and rN-CM (E–H). Each panel shows I_{NCX} during spontaneous oscillations at the top and responses to paired caffeine exposures (3 mM) at the bottom. The four panels illustrating each cell type show results under control conditions (A and E) and the gradual effects of exposure of hiPS-CM to 0.5 μM thapsigargin for 5 min (B), 8 min (C) and 10 min (D) or rN-CM to 5 μM thapsigargin for 3 min (F), 5 min (G) and 7 min (H). Cells were voltage-clamped at 24 °C at a holding potential of −50 mV, and dialyzed with a solution containing 0.1 mM EGTA.

Please cite this article in press as: X.-H. Zhang, et al., Regionally diverse mitochondrial calcium signaling regulates spontaneous pacing in developing cardiomyocytes, Cell Calcium (2015), http://dx.doi.org/10.1016/j.ceca.2015.02.003

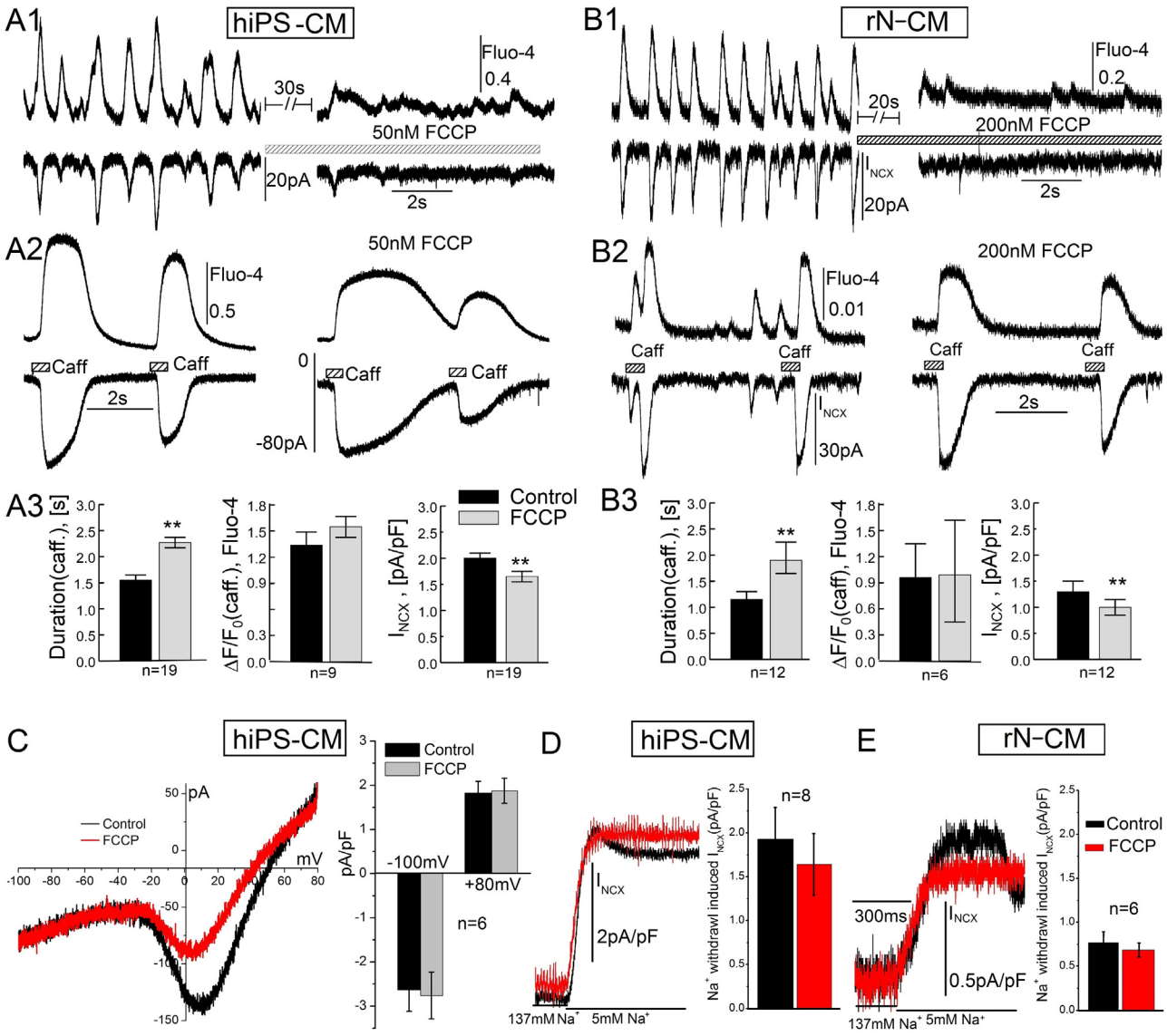

Fig. 12. Suppression of spontaneous beating by the mitochondrial uncoupler FCCP. (A1)–(A3) (hiPS-CM, 50 nM FCCP) and (B1)–(B3) (rN-CM, 200 nM FCCP): Matched tracings of Ca^{2+}-signals (Fluo-4) and membrane current (I_{NCX}) showing strong suppression of spontaneous Ca^{2+} and I_{NCX} oscillations (A1 and B1), but prolongation of the caffeine-induced (3 mM) signals (A2 and B2) with only minor changes in their amplitudes (A3 and B3). (C) Ramp-clamp data suggesting that 100 nM FCCP slightly attenuated I_{Ca} (in the range −30 to 40 mV) without affecting I_{NCX}. The histograms show that 100 nM FCCP had no significant effects on the current measured at −100 and +80 mV. (D) and (E) I_{NCX} measured in response to Na^+-withdrawal (137 → 5 mM; TEA substitution) before (black) and after (red) treatment with FCCP in hiPS-CM (D) and rN-CM (E). The cells were voltage-clamped at 24 °C and dialyzed with a solution containing 100 μM Fluo-4 (A and B) or EGTA (C–E).

This raises the question as to the role of I_f current in mouse and human iPS-CM, as it is present in these cells (Fig. 7), and in mammalian SA-node, where it is proposed to initiate diastolic depolarization alone [3] or together with Ca^{2+}-activated I_{NCX} [7]. It is a somewhat of over-looked observation that in SA-nodal cells too, including human [48], there is a discrepancy between diastolic depolarization potentials (−60 to −40 mV) and activation range of I_f (negative to −70 mV). A combination of rapid 2-D Ca^{2+} imaging and voltage- and current-clamp studies might clarify the role of I_f in SA-nodal cells by examining whether sub-sarcolemmal Ca^{2+} transients always precede the diastolic depolarization. We suggest that I_f is critical in protecting the small pacemaker cells from the large voltage sink of bigger atrial cells by serving as a "*functional insulator*". It is likely that without expression of HCN proteins, activating strongly and rapidly at potentials near the atrial resting potentials (~−90 mV), the SA-nodal cells would be hyperpolarized to more negative resting potentials of atrium, thereby preventing them from generating the diastolic depolarization necessary for pacing the heart. This property of I_f along with significantly lower expression of I_{K1} channels especially in SA-nodal/atrial junctional cells may serve as a dynamic "push-me pull-you" current oscillations that might amplify the oscillations set by the Ca^{2+} signaling mechanisms in central SA-nodal cells.

4.2. *Rhythmic spontaneous Ca^{2+} release and NCX current oscillations*

The central observation of this report is that spontaneous rhythmic oscillations of cytosolic Ca^{2+} and the accompanying I_{NCX} were consistently recorded in myocytes that were voltage-clamped at constant holding potentials of −50 mV, where no ionic channels were allowed to activate (Figs. 1–5 and 7–14). The sensitivity of these signals to KB-R7943, Ni^{2+} and Cd^{2+} suggest that the current oscillations (I_{NCX}) were triggered by cytosolic Ca^{2+} changes

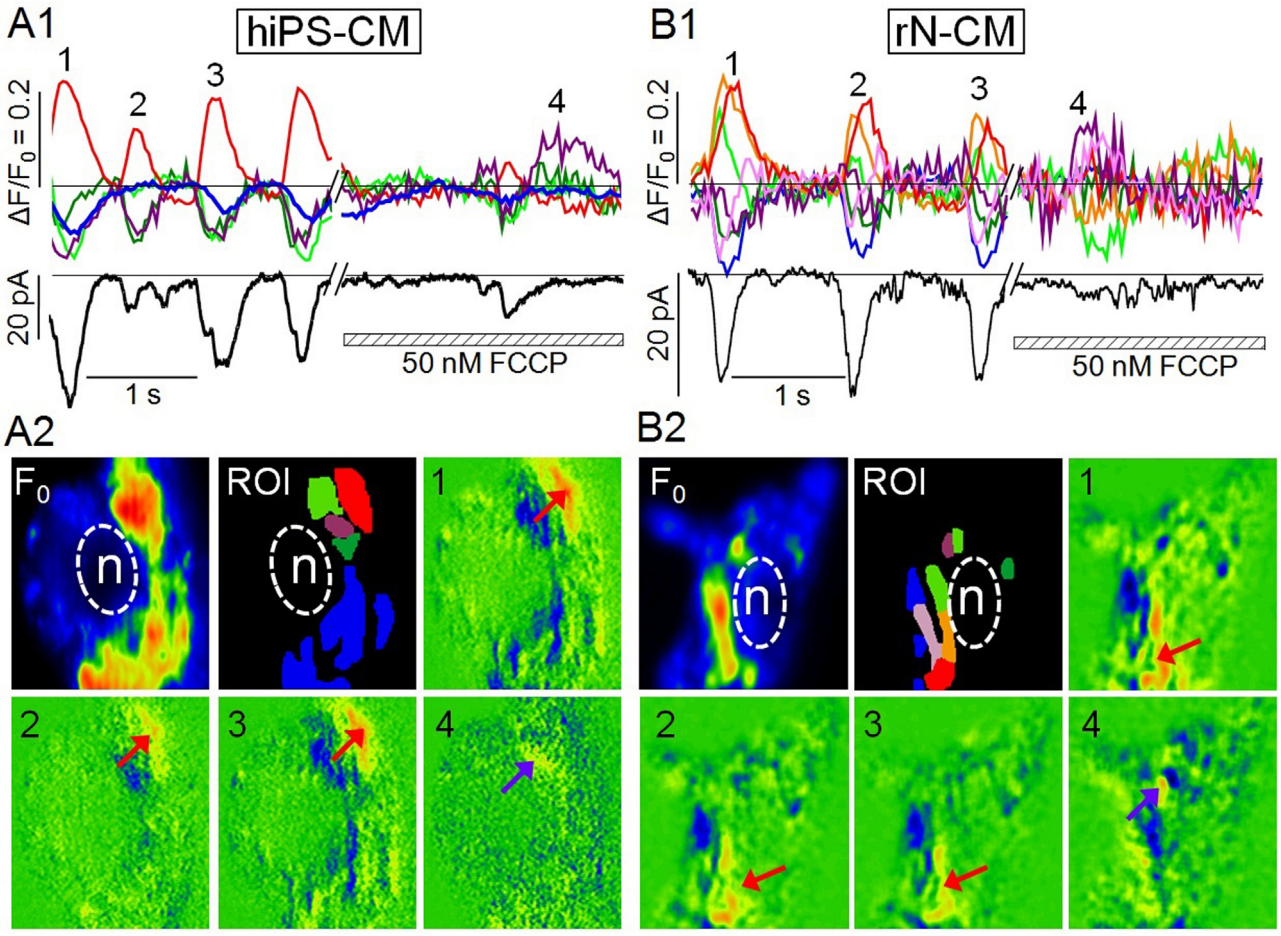

Fig. 13. Suppression of mitochondrial Ca^{2+} oscillations by FCCP in myticam-E31Q infected hiPS-CM (A1 and A2) and rN-CM (B1 and B2). The tracings show changes in regional mitochondrial Ca^{2+} signals (top) and I_{NCX} (bottom) before and 30 s after exposure to 50 nM FCCP (A1 and B1). For each cell type the images (A2 and B2) show baseline fluorescence (F_0) and color-coded regions of interest (ROI, with "n" indicating nuclei) and 4 differential fluorescence images (measured at the times indicated along the traces) showing repeatable mitochondial Ca^{2+} signals before FCCP application (1, 2, 3) and smaller, more localized responses after (4). Increases in mitycam-E31Q fluorescence (reddish hues, arrows) correspond to reduced mitochondrial Ca^{2+}, *i.e.* mitochondrial Ca^{2+} release. The cells were voltage-clamped at 24 °C and dialyzed with a solution containing 100 μM EGTA, while 2-D confocal imaging at 30 Hz was used simultaneously to measure mitochondrial Ca^{2+} reported by myticam-E31Q.

activating the NCX current (Fig. 9). Although the rhythmic activity was fairly constant, either at the onset of dialysis and before imaging laser light, they became more irregular following exposure to intense light of confocal imaging. Such irregularities were less apparent when imaging measurements were not attempted. Confocal examination of such rhythmic beating activity in cells dialyzed with Fluo-4 and held at −60 or −50 mV suggests multiple Ca^{2+} release sites. The stronger Ca^{2+} triggering sites appeared to invade the cell rapidly and fully (Figs. 4–6) while weaker sites were not able to invade the cell fully (Figs. 5 and 6). It is not clear as yet why the strong triggering sites give way to the weaker site, but since the frequency of spontaneously occurring rhythmic activity is not significantly altered by nifedipine (Fig. 8) or by holding potentials (−60 to 0 mV; Fig. 3), the data is consistent with activation of different Ca^{2+} pools capable of maintaining the rhythmic activity.

The Ca^{2+}-dependent mechanism described here for two types of developing cells provides the intriguing possibility that significant rises of Ca^{2+} may occur in specific cellular micro-domains of the spontaneously pacing cell during diastolic depolarization, prior to activation of upstroke of the action potential (Figs. 2 and 4) that may in turn contribute to slow diastolic depolarization of the membrane. This mechanism might be somewhat different from that described for the adult SA-nodal cells where voltage-gated channels are thought to play a mandatory role [7,18,49]. It remains to be explored whether these differences are associated with the developmental stages of the examined cells or experimental approaches.

4.3. *Nature of Ca^{2+} pools supporting the spontaneous rhythmic beating*

The findings that tetracaine and thapsigargin suppressed the rhythmic beating in both hiPS-CM and rN-CM (Figs. 10 and 11) suggests Ca^{2+} release from the SR is critical in generating the rhythmic beating. Somewhat less expected were the rapid and reversible suppressive effects of small (50–100 nM) and short exposures to mitochondrial un-coupler FCCP on the rhythmic activity (Figs. 12 and 13). Since FCCP also suppressed the rate of relaxation of caffeine-triggered Ca^{2+}-transients (Figs. 12 and 14) as it inhibited the mitochondrial Ca^{2+} signals associated with spontaneous pacing (Figs. 12 and 13), the data suggests a critical role for mitochondria in spontaneous pacing. The mitochondrial imaging experiments with mitycam-E31Q probe, suggesting that the perinuclear population of mitochondria release Ca^{2+} as the peripheral mitochondria take up Ca^{2+} (Fig. 13, spontaneous beating and Fig. 14, caffeine application), were somewhat surprising, but do provide an intriguing possibility that may couple the mitochondrial ATP production to the rhythmic Ca^{2+} signaling and spontaneous beating. It is not as yet clear whether Ca^{2+} sequestered by mitochondrial is

Please cite this article in press as: X.-H. Zhang, et al., Regionally diverse mitochondrial calcium signaling regulates spontaneous pacing in developing cardiomyocytes, Cell Calcium (2015), http://dx.doi.org/10.1016/j.ceca.2015.02.003

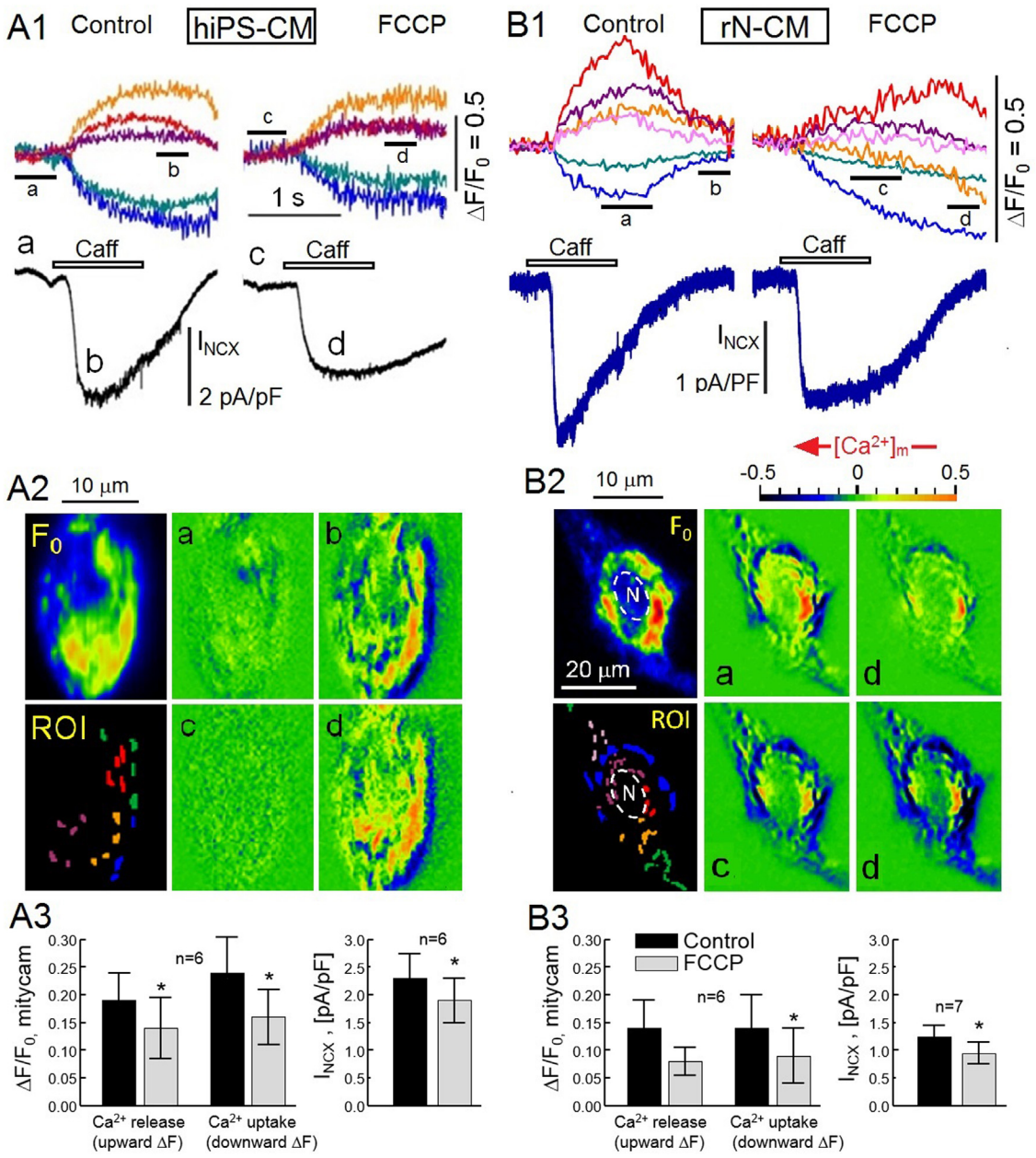

Fig. 14. Suppression of regional caffeine-induced regional mitochondrial Ca^{2+} signals by FCCP in a hiPS-CM (A1–A3) and rN-CM (B1–B3). (A1) and (B1) Time course of changes of fluorescence intensities in color-coded ROIs and I_{NCX} before (Control) and after addition of 50 nM FCCP. (A2) and (B2) Baseline fluorescence (F_0), ROIs (ROI), and changes in mitochondrial Ca^{2+} the times (a–d) indicated along the I_{NCX} trace. The cell was incubated in 10 μM blebbistatin to suppress cell shortening. (A3) and (B3) Average values of I_{NCX} and of mitochondrial Ca^{2+} uptake and release measured in the most active regions of rN-CM and hiPS-CM. The cells were voltage-clamped at 24 °C and dialyzed with a solution containing 100 μM EGTA, while 2-D confocal imaging at 30 Hz was used simultaneously to measure mitochondrial Ca^{2+} reported by myticam-E31Q with a decrease in fluorescence.

re-released directly into the cytosol or is transferred *via* specialized SR-mitochondrial junctions into the SR, and thereby modulating spontaneous beating. Our data clearly provide some support for mitochondrial Ca^{2+} release (Figs. 13–14), but the release mechanism remains unclear, though proposed candidates range from mitochondrial permeability transition pore (mPTP), and mNCX, to mRyR1 [50–52].

4.4. Physiological implications

Rhythmic activity in the adult mammalian heart originates from the SA-nodal cells. The morphology of SA-nodal cells differs sharply from their neighboring atrial and ventricular cells. They are smaller, ~20 pF *vs.* 70–250 pF for atrial and ventricular cells, with large surface to volume ratios, allowing for released Ca^{2+} to produce larger local Ca^{2+} concentrations, activating thereby larger inward I_{NCX}. Spontaneously beating rN-CM and hiPS-CM are similarly small (~20 pF), with large surface/volume ratios, and robust Ca^{2+} releases generating large I_{NCX} (Figs. 1–5 and 7–13). Interestingly, unlike hiPS-CM, rN-CM do not express I_f, yet have higher pacing frequency, and otherwise are indistinguishable from hiPS-CM electrophysiologically, supporting the idea of minor role for I_f in spontaneous pacing of developing cardiomyocytes

Our studies provide insight into the mechanism that sets the "Ca^{2+} oscillator" in developing cardiomyocytes. Clearly depletion of Ca^{2+} content of SR, using caffeine or thapsigargin (Fig. 11), or blocking the RyRs (Fig. 10) stops the rhythmic Ca^{2+} oscillations, implicating the SR Ca^{2+} release to be critical in initiation of rhythmic

beating. More intriguing, however, is the finding that short exposures of 50 nM FCCP, reported to enhance oxidative metabolism, but not to depolarize the mitochondria or reduce ATP levels [30], consistently blocked the rhythmic activity rapidly and reversibly. Since the drug prolonged the rate of re-uptake of Ca^{2+} of spontaneously activated or caffeine-triggered Ca^{2+} transients (Fig. 12), it is likely that mitochondria have a critical role in rhythmic Ca^{2+}-cycling thus modulating pacemaker activity in developing myocytes. We suggest that a cross-talk between SR and mitochondria sets the rhythmic cycle of Ca^{2+} release and re-uptake that results in cyclic activation of NCX to generate the inward current necessary to depolarize the myocyte at voltages beyond the activation voltage of I_f (Fig. 7). This possibility is strongly supported by the perforated patch and current-clamped experiments where the pacing cell generates significant rises of Ca^{2+} in specific cellular micro-domains prior to the upstroke of the action potential at −50 mV (see Fig. 2).

Experiments using mitycam-infected cells show diversity in mitochondrial populations *vis-à-vis* Ca^{2+} release and uptake. In this respect FCCP was effective in suppressing both the mitochondrial release and uptake signals as it suppressed the spontaneous beating and I_{NCX} accompanying them (Fig. 13). It is likely that this diversity in Ca^{2+}-signaling of different mitochondrial populations serves as an additional oscillatory mechanism contributing to spontaneous pacing. Whether the processes that generate spontaneous pacing are also coupled to the energy producing mechanisms remains to be explored. This possibility may reinforce the notion that Ca^{2+} signaling parameters are relevant to normal and abnormal cardiac impulse formation where mitochondrial dysfunction may play a critical role in pathologies like arrhythmias and dilated cardiomyopathy [53].

5. Conclusions

Regionally diverse mitochondrial Ca^{2+}-signaling, in addition to RyR2/NCX co-activation, may provide the critical negative feedback mechanism that initiates and regulates spontaneous beating in developing cardiomyocytes, independent of I_f-channels.

Conflict of interest

None of the authors have any actual or potential conflict of interest including any financial, personal or other relationships with other people or organizations within three years of beginning the submitted work that could inappropriately influence, or be perceived to influence, their work.

Acknowledgements

We thank Drs. Naohiro Yamaguchi and Sara Pahlavan for constructing the FKBP-linked GCamP6 Ca^{2+} probe and making it available to us. This study was supported by grants to MM (NIH R01 HL15162 and R01 HL107600) and TS (BMBF 01GN0824).

Appendix A. Supplementary data

Supplementary data associated with this article can be found, in the online version, at http://dx.doi.org/10.1016/j.ceca.2015.02.003.

References

[1] J. Maylie, M. Morad, J. Weiss, A study of pace-maker potential in rabbit sino-atrial node: measurement of potassium activity under voltage-clamp conditions, J. Physiol. 311 (1981) 161–178.
[2] K. Yanagihara, H. Irisawa, Inward current activated during hyperpolarization in the rabbit sinoatrial node cell, Pflugers Arch. 385 (1980) 11–19.
[3] H. Brown, D. Difrancesco, Voltage-clamp investigations of membrane currents underlying pace-maker activity in rabbit sino-atrial node, J. Physiol. 308 (1980) 331–351.
[4] A. Ludwig, X. Zong, M. Jeglitsch, F. Hofmann, M. Biel, A family of hyperpolarization-activated mammalian cation channels, Nature 393 (1998) 587–591.
[5] W. Shi, R. Wymore, H. Yu, J. Wu, R.T. Wymore, Z. Pan, R.B. Robinson, J.E. Dixon, D. McKinnon, I.S. Cohen, Distribution and prevalence of hyperpolarization-activated cation channel (HCN) mRNA expression in cardiac tissues, Circ. Res. 85 (1999) e1–e6.
[6] Y.K. Ju, D.G. Allen, Intracellular calcium and Na+-Ca2+ exchange current in isolated toad pacemaker cells, J. Physiol. 508 (Pt 1) (1998) 153–166.
[7] K.Y. Bogdanov, T.M. Vinogradova, E.G. Lakatta, Sinoatrial nodal cell ryanodine receptor and Na(+)-Ca(2+) exchanger: molecular partners in pacemaker regulation, Circ. Res. 88 (2001) 1254–1258.
[8] L. Sanders, S. Rakovic, M. Lowe, P.A. Mattick, D.A. Terrar, Fundamental importance of Na+-Ca2+ exchange for the pacemaking mechanism in guinea-pig sino-atrial node, J. Physiol. 571 (2006) 639–649.
[9] M. Vassalle, Analysis of cardiac pacemaker potential using a voltage clamp technique, Am. J. Physiol. 210 (1966) 1335–1341.
[10] D. Noble, R.W. Tsien, The kinetics and rectifier properties of the slow potassium current in cardiac Purkinje fibres, J. Physiol. 195 (1968) 185–214.
[11] W. Trautwein, D.G. Kassebaum, On the mechanism of spontaneous impulse generation in the pacemaker of the heart, J. Gen. Physiol. 45 (1961) 317–330.
[12] R. Sakai, N. Hagiwara, N. Matsuda, H. Kassanuki, S. Hosoda, Sodium–potassium pump current in rabbit sino-atrial node cells, J. Physiol. 490 (Pt 1) (1996) 51–62.
[13] D. Noble, S.J. Noble, A model of sino-atrial node electrical activity based on a modification of the DiFrancesco–Noble (1984) equations, Proc. R. Soc. Lond. B: Biol. Sci. 222 (1984) 295–304.
[14] E.G. Lakatta, V.A. Maltsev, T.M. Vinogradova, A coupled SYSTEM of intracellular Ca2+ clocks and surface membrane voltage clocks controls the timekeeping mechanism of the heart's pacemaker, Circ. Res. 106 (2010) 659–673.
[15] T.A. Quinn, P. Kohl, Mechano-sensitivity of cardiac pacemaker function: pathophysiological relevance, experimental implications, and conceptual integration with other mechanisms of rhythmicity, Prog. Biophys. Mol. Biol. 110 (2012) 257–268.
[16] S. Belmonte, M. Morad, Shear fluid-induced Ca2+ release and the role of mitochondria in rat cardiac myocytes, Ann. N. Y. Acad. Sci. 1123 (2008) 58–63.
[17] A. Takeuchi, B. Kim, S. Matsuoka, The mitochondrial Na+-Ca2+ exchanger, NCLX, regulates automaticity of HL-1 cardiomyocytes, Sci. Rep. 3 (2013) 2766.
[18] Y. Yaniv, H.A. Spurgeon, A.E. Lyashkov, D. Yang, B.D. Ziman, V.A. Maltsev, E.G. Lakatta, Crosstalk between mitochondrial and sarcoplasmic reticulum Ca2+ cycling modulates cardiac pacemaker cell automaticity, PLoS ONE 7 (2012) e37582.
[19] D.A. Brown, B. O'Rourke, Cardiac mitochondria and arrhythmias, Cardiovasc. Res. 88 (2010) 241–249.
[20] T.M. Vinogradova, Y.Y. Zhou, V. Maltsev, A. Lyashkov, M. Stern, E.G. Lakatta, Rhythmic ryanodine receptor Ca2+ releases during diastolic depolarization of sinoatrial pacemaker cells do not require membrane depolarization, Circ. Res. 94 (2004) 802–809.
[21] G.S. Williams, L. Boyman, A.C. Chikando, R.J. Khairallah, W.J. Lederer, Mitochondrial calcium uptake, Proc. Natl. Acad. Sci. U. S. A. 110 (2013) 10479–10486.
[22] M. Wang, L. Jiang, R.E. Monticone, E.G. Lakatta, Proinflammation: the key to arterial aging, Trends Endocrinol. Metab. 25 (2014) 72–79.
[23] T. Saric, M. Halbach, M. Khalil, F. Er, Induced pluripotent stem cells as cardiac arrhythmic in vitro models and the impact for drug discovery, Expert Opin. Drug Discov. 9 (2014) 55–76.
[24] M.K. Gupta, D.J. Illich, A. Gaarz, M. Matzkies, F. Nguemo, K. Pfannkuche, H. Liang, S. Classen, M. Reppel, J.L. Schultze, J. Hescheler, T. Saric, Global transcriptional profiles of beating clusters derived from human induced pluripotent stem cells and embryonic stem cells are highly similar, BMC Dev. Biol. 10 (2010) 98.
[25] A. Fatima, G. Xu, K. Shao, S. Papadopoulos, M. Lehmann, J.J. Arnaiz-Cot, A.O. Rosa, F. Nguemo, M. Matzkies, S. Dittmann, S.L. Stone, M. Linke, U. Zechner, V. Beyer, H.C. Hennies, S. Rosenkranz, B. Klauke, A.S. Parwani, W. Haverkamp, G. Pfitzer, M. Farr, L. Cleemann, M. Morad, H. Milting, J. Hescheler, T. Saric, In vitro modeling of ryanodine receptor 2 dysfunction using human induced pluripotent stem cells, Cell. Physiol. Biochem. 28 (2011) 579–592.
[26] X.H. Zhang, S. Haviland, H. Wei, T. Saric, A. Fatima, J. Hescheler, L. Cleemann, M. Morad, Ca2+ signaling in human induced pluripotent stem cell-derived cardiomyocytes (iPS-CM) from normal and catecholaminergic polymorphic ventricular tachycardia (CPVT)-afflicted subjects, Cell Calcium 54 (2013) 57–70.
[27] T.W. Chen, T.J. Wardill, Y. Sun, S.R. Pulver, S.L. Renninger, A. Baohan, E.R. Schreiter, R.A. Kerr, M.B. Orger, V. Jayaraman, L.L. Looger, K. Svoboda, D.S. Kim, Ultrasensitive fluorescent proteins for imaging neuronal activity, Nature 499 (2013) 295–300.
[28] S. Haviland, L. Cleemann, S. Kettlewell, G.L. Smith, M. Morad, Diversity of mitochondrial Ca(2)(+) signaling in rat neonatal cardiomyocytes: evidence from a genetically directed Ca(2)(+) probe, mitycam-E31Q, Cell Calcium 56 (2014) 133–146.
[29] V.V. Fedorov, I.T. Lozinsky, E.A. Sosunov, E.P. Anyukhovsky, M.R. Rosen, C.W. Balke, I.R. Efimov, Application of blebbistatin as an excitation-contraction uncoupler for electrophysiologic study of rat and rabbit hearts, Heart Rhythm 4 (2007) 619–626.
[30] J.P. Brennan, R.G. Berry, M. Baghai, M.R. Duchen, M.J. Shattock, FCCP is cardioprotective at concentrations that cause mitochondrial oxidation without detectable depolarisation, Cardiovasc. Res. 72 (2006) 322–330.

Please cite this article in press as: X.-H. Zhang, et al., Regionally diverse mitochondrial calcium signaling regulates spontaneous pacing in developing cardiomyocytes, Cell Calcium (2015), http://dx.doi.org/10.1016/j.ceca.2015.02.003

[31] E. Janowski, M. Berrios, L. Cleemann, M. Morad, Developmental aspects of cardiac Ca(2+) signaling: interplay between RyR- and IP(3)R-gated Ca(2+) stores, Am. J. Physiol. Heart Circ. Physiol. 298 (2010) H1939–H1950.
[32] K. Takahashi, K. Tanabe, M. Ohnuki, M. Narita, T. Ichisaka, K. Tomoda, S. Yamanaka, Induction of pluripotent stem cells from adult human fibroblasts by defined factors, Cell 131 (2007) 861–872.
[33] C. Mummery, D. Ward-van Oostwaard, P. Doevendans, R. Spijker, S. van den Brink, R. Hassink, M. van der Heyden, T. Opthof, M. Pera, A.B. de la Riviere, R. Passier, L. Tertoolen, Differentiation of human embryonic stem cells to cardiomyocytes: role of coculture with visceral endoderm-like cells, Circulation 107 (2003) 2733–2740.
[34] M. Halbach, G. Peinkofer, S. Baumgartner, M. Maass, M. Wiedey, K. Neef, B. Krausgrill, D. Ladage, A. Fatima, T. Saric, J. Hescheler, J. Muller-Ehmsen, Electrophysiological integration and action potential properties of transplanted cardiomyocytes derived from induced pluripotent stem cells, Cardiovasc. Res. 100 (2013) 432–440.
[35] M. Rubach, R. Adelmann, M. Haustein, F. Drey, K. Pfannkuche, B. Xiao, A. Koester, F.E. Udink ten Cate, Y.H. Choi, K. Neef, A. Fatima, T. Hannes, F. Pillekamp, J. Hescheler, T. Saric, K. Brockmeier, M. Khalil, Mesenchymal stem cells and their conditioned medium improve integration of purified induced pluripotent stem cell-derived cardiomyocyte clusters into myocardial tissue, Stem Cells Dev. 23 (2014) 643–653.
[36] L. Cleemann, W. Wang, M. Morad, Two-dimensional confocal images of organization, density, and gating of focal Ca2+ release sites in rat cardiac myocytes, Proc. Natl. Acad. Sci. U. S. A. 95 (1998) 10984–10989.
[37] A. Noma, M. Morad, H. Irisawa, Does the pacemaker current generate the diastolic depolarization in the rabbit SA node cells? Pflugers Arch. 397 (1983) 190–194.
[38] A. Bucchi, M. Baruscotti, D. DiFrancesco, Current-dependent block of rabbit sino-atrial node I(f) channels by ivabradine, J. Gen. Physiol. 120 (2002) 1–13.
[39] Y. Kurata, I. Hisatome, S. Imanishi, T. Shibamoto, Roles of L-type Ca2+ and delayed-rectifier K+ currents in sinoatrial node pacemaking: insights from stability and bifurcation analyses of a mathematical model, Am. J. Physiol. Heart Circ. Physiol. 285 (2003) H2804–H2819.
[40] I. Itzhaki, S. Rapoport, I. Huber, I. Mizrahi, L. Zwi-Dantsis, G. Arbel, J. Schiller, L. Gepstein, Calcium handling in human induced pluripotent stem cell derived cardiomyocytes, PLoS ONE 6 (2011) e18037.
[41] I. Zahanich, S.G. Sirenko, L.A. Maltseva, Y.S. Tarasova, H.A. Spurgeon, K.R. Boheler, M.D. Stern, E.G. Lakatta, V.A. Maltsev, Rhythmic beating of stem cell-derived cardiac cells requires dynamic coupling of electrophysiology and Ca cycling, J. Mol. Cell. Cardiol. 50 (2011) 66–76.
[42] S. Adachi-Akahane, L. Lu, Z. Li, J.S. Frank, K.D. Philipson, M. Morad, Calcium signaling in transgenic mice overexpressing cardiac Na(+)-Ca2+ exchanger, J. Gen. Physiol. 109 (1997) 717–729.
[43] C.A. Mason, G.R. Ferrier, Tetracaine can inhibit contractions initiated by a voltage-sensitive release mechanism in guinea-pig ventricular myocytes, J. Physiol. 519 (3) (1999) 851–865.
[44] J. Schaper, E. Meiser, G. Stammler, Ultrastructural morphometric analysis of myocardium from dogs, rats, hamsters, mice, and from human hearts, Circ. Res. 56 (1985) 377–391.
[45] I. Drago, D. De Stefani, R. Rizzuto, T. Pozzan, Mitochondrial Ca2+ uptake contributes to buffering cytoplasmic Ca2+ peaks in cardiomyocytes, Proc. Natl. Acad. Sci. U. S. A. 109 (2012) 12986–12991.
[46] S. Kettlewell, P. Cabrero, S.A. Nicklin, J.A. Dow, S. Davies, G.L. Smith, Changes of intra-mitochondrial Ca2+ in adult ventricular cardiomyocytes examined using a novel fluorescent Ca2+ indicator targeted to mitochondria, J. Mol. Cell. Cardiol. 46 (2009) 891–901.
[47] J. Maylie, M. Morad, Ionic currents responsible for the generation of pace-maker current in the rabbit sino-atrial node, J. Physiol. 355 (1984) 215–235.
[48] A.O. Verkerk, R. Wilders, M.M. van Borren, R.J. Peters, E. Broekhuis, K. Lam, R. Coronel, J.M. de Bakker, H.L. Tan, Pacemaker current (I(f)) in the human sinoatrial node, Eur. Heart J. 28 (2007) 2472–2478.
[49] M.D. Stern, L.A. Maltseva, M. Juhaszova, S.J. Sollott, E.G. Lakatta, V.A. Maltsev, Hierarchical clustering of ryanodine receptors enables emergence of a calcium clock in sinoatrial node cells, J. Gen. Physiol. 143 (2014) 577–604.
[50] T.E. Gunter, L. Buntinas, G. Sparagna, R. Eliseev, K. Gunter, Mitochondrial calcium transport: mechanisms and functions, Cell Calcium 28 (2000) 285–296.
[51] Y. Kirichok, G. Krapivinsky, D.E. Clapham, The mitochondrial calcium uniporter is a highly selective ion channel, Nature 427 (2004) 360–364.
[52] B.A. Altschafl, G. Beutner, V.K. Sharma, S.S. Sheu, H.H. Valdivia, The mitochondrial ryanodine receptor in rat heart: a pharmaco-kinetic profile, Biochim. Biophys. Acta 1768 (2007) 1784–1795.
[53] P. Rosenberg, Mitochondrial dysfunction and heart disease, Mitochondrion 4 (2004) 621–628.

Xiao-Hua Zhang works in the laboratories of the Cardiac Signaling center in Charleston, South Carolina, where she performed almost all the reported voltage-clamp and Ca^{2+} imaging experiments and has had a leading role in the analysis of data and preparation of the manuscript.

Hua Wei works in the laboratories of the Cardiac Signaling center in Charleston, South Carolina, where he has generated and maintenaned of hiPS-CM and miPS-CM cultures.

Tomo Šarić works at the University of Cologne, Germany, where he was instrumental in transfecting somatic human cells with pluripotency genes and guiding their differentiation to a stable cardiac phenotype.

Jürgen Hescheler works at the University of Cologne, Germany, where he was instrumental in transfecting somatic human cells with pluripotency genes and guiding their differentiation to a stable cardiac phenotype.

Lars Cleemann works in the laboratories of the Cardiac Signaling Center in Charleston, South Carolina, USA, where he took part in the instrumentation and experimentation. He has played a major role in formalizing and executing the evaluation of data and their graphic presentation in figures and in the preparation of the final manuscript.

Martin Morad works in the laboratories of the Cardiac Signaling Center in Charleston, South Carolina, USA. He played a major role in the conception and design of the experiments and in the drafting of the manuscript. He has supervised the project and taken part in the analysis of and evaluation of data.

Please cite this article in press as: X.-H. Zhang, et al., Regionally diverse mitochondrial calcium signaling regulates spontaneous pacing in developing cardiomyocytes, Cell Calcium (2015), http://dx.doi.org/10.1016/j.ceca.2015.02.003